LSI ER-258-10
CR-151995

TECHNOLOGY ADVANCEMENT OF THE ELECTROCHEMICAL CO_2 CONCENTRATING PROCESS

ANNUAL REPORT

by

F. H. Schubert, R. R. Woods,
T. M. Hallick and D. B. Heppner

May, 1977

Prepared Under Contract NAS2-8666

by

Life Systems, Inc.
Cleveland, Ohio 44122

for

AMES RESEARCH CENTER
National Aeronautics and Space Administration

National Aeronautics and
Space Administration

Ames Research Center
Moffett Field, California
94035

NASA

Reply to Attn of NAS 2-8666
ATL:202-3

August 8, 1977

NASA Representative
Scientific & Technical Information Facility
P.O. Box 8757
Baltimore/Washington International Airport
Maryland 21240

Subject: Transmittal of Contractor Report: "Technology Advancement of the Electrochemical CO_2 Concentrating Process," Annual Report, dated May 1977, by F.H. Schubert, R.R. Woods, T. M. Hallick and D.B. Heppner, Life Systems, Inc., Cleveland, Ohio 44122.

Reference: Program Code 199-73-02-05

The subject report prepared under Contract NAS2-8666 has been reviewed at Ames and is recommended for release in STAR as CR-151995.

Ralph W. Lewis
Chief, Library Branch

Enclosure:
1 cy subject report

cc:
NASA Hqrs., Code KSI (w/o encs.)

ER-258-10

TECHNOLOGY ADVANCEMENT OF THE ELECTROCHEMICAL CARBON DIOXIDE CONCENTRATING PROCESS

ANNUAL REPORT

by

F. H. Schubert, R. R. Woods,
T. M. Hallick and D. B. Heppner

May, 1977

Prepared Under Contract NAS2-8666

by

Life Systems, Inc.
Cleveland, OH 44122

for

Ames Research Center
National Aeronautics and Space Administration

FOREWORD

The development work described herein was conducted by Life Systems, Inc. at Cleveland, Ohio under Contract NAS2-8666, during the period of February, 1975 through March, 1977. All program activities are scheduled for completion by May, 1979. The Program Manager was Franz H. Schubert. The personnel contributing to the program and their responsibilities are outlined below:

Personnel	Area of Responsibility
Ron J. Davenport, Ph.D.	Electrode Kinetic Studies
Tim M. Hallick	Program Testing, Data Reduction, Module Cell Configuration
Dennis B. Heppner, Ph.D	Liquid/Gas Separator, Air Supply Unit Design
Fred C. Jensen	Mechanical Component and System Design
Michael L. Kruszynski	Mechanical Component/System Assembly and Checkout
Richard D. Marshall	System Integration, Electrochemical Design
Jim J. Palagyi	Electronic Assembly and Checkout
J. David Powell	Control and Monitor Instrumentation and Sensing Design
Franz H. Schubert	Program Manager, System Analysis and Design
John W. Shumar	Product Assurance, Electrode/Matrix Development
Daniel C. Walter	Mechanical Design
Richard R. Woods, Jr.	Electrolyte Mixture Studies, Electrochemical and Chemical Performance Analysis
Rick A. Wynveen, Ph.D.	Program Administration, Electrochemical Support Concept Evaluations

The contract's Technical Monitor was P. D. Quattrone, Chief, Advanced Life Support Project Office, NASA Ames Research Center, Moffett Field, CA.

TABLE OF CONTENTS

LIST OF FIGURES

LIST OF TABLES

LIST OF ACRONYMS

ARS	Air Revitalization System
ASU	Air Supply Unit
BRS	Bosch Reduction Subsystem
CSU	Coolant Supply Unit
CS-6	Six-Man, SSP CO_2 Concentrator Subsystem
CX-1	One-Man, Self-Contained CO_2 Concentrating Subsystem
CXA-4(A)	Four-Man Capacity Air-Cooled EDC
EC/LSS	Environmental Control/Life Support Subsystem
EDC	Electrochemical Depolarized CO_2 Concentrator
FSU	Fluid Supply Unit
LBS-B/ORS-4(A)	Laboratory Breadboard Bosch-Based O_2 Reclamation System Four-Man Level
LBS-S/ORS-1(L)	One-Man Laboratory Breadboard Sabatier-Based O_2 Reclamation Subsystem
NSS	Nitrogen Supply Subsystem
OGS	Oxygen Generation System
ORS	Oxygen Reclamation Subsystem
S-CRS	Sabatier-Based CO_2 Reduction Subsystem
SSP	Space Station Prototype
TACU	Test Accessories Control Unit
TSA	Test Support Accessories

SUMMARY

Regenerative carbon dioxide removal concepts are needed to sustain man in space for extended periods of time. A program to develop an electrochemical carbon dioxide concentration technique has been underway at the National Aeronautics and Space Administration and Life Systems, Inc. for the past several years. The work reported herein, Technology Advancement of the Electrochemical Carbon Dioxide Concentrating Process, is a portion of the overall program.

Activities in five major areas were successfully completed:

1. Further development of the liquid-cooled advanced Electrochemical Depolarized Carbon Dioxide Concentrator including the fabrication of a one-man capacity liquid-cooled module.

2. Testing of the advanced liquid-cooled Electrochemical Depolarized Carbon Dioxide Concentrator integrated in a laboratory breadboard Oxygen Generation and Recovery System.

3. Component development and testing to support the fabrication of a process air conditioning and humidity control subsystem for one-man Electrochemical Depolarized Carbon Dioxide Concentrator testing.

4. Development of Test Support Accessories to support single cell and subsystem level testing of Electrochemical Depolarized Carbon Dioxide Concentrators.

5. Technology advancement studies of the basic electrochemical carbon dioxide removal processes to provide a basis for the design of the next generation cell, module and subsystem hardware.

A five-cell, liquid-cooled advanced Electrochemical Depolarized Carbon Dioxide Concentrator Module was fabricated. The cells utilized the advanced, lightweight, plated anode current collector concept and internal liquid-cooling. The five cell module was designed to meet the carbon dioxide removal requirements of one man and was assembled using plexiglass endplates. This one-man module was tested as part of an integrated Oxygen Generation and Recovery Subsystem.

Subsystem integration support activities were performed in conjunction with two laboratory breadboard system tests. One test combined the liquid-cooled advanced Electrochemical Depolarized Carbon Dioxide Concentrator Module an Oxygen Generation Subsystem and a Carbon Dioxide Reduction Subsystem based on a Sabatier reactor. A 30-day test of this Oxygen Generation and Recovery System was performed. The test demonstrated the long-term, multi-cell, liquid-cooled advanced Electrochemical Depolarized Carbon Dioxide Concentrator Module operation and verified satisfactory operation with the hydrogen generated by the Oxygen Generation Subsystem. At an operating current density of 30.1 mA/cm^2 (28 ASF) the average cell voltages obtained were 0.4 V for the Electrochemical Depolarized Carbon Dioxide Concentrator and the module exhibited an average transfer efficiency of 76% for the duration of the test. The Sabatier reactor

also demonstrated efficient operation with the Electrochemical Carbon Dioxide Concentrator exhaust gas. The hydrogen conversion efficiency of the Sabatier reactor throughout the testing averaged 97%.

The second laboratory breadboard test consisted of a four-man capacity air-cooled Electrochemical Depolarized Carbon Dioxide Concentrator, a Bosch-based Carbon Dioxide Reduction System and an Oxygen Generation Subsystem. Integrated checkout and shakedown testing of this combined system has been successfully completed. Endurance testing for up to 30 days is scheduled for the next reporting period.

Several components were developed as part of an Electrochemical Depolarized Carbon Dioxide Concentrator process air conditioning and humidity control hardware. These hardware items are required to permit simulation of the interface between the Electrochemical Depolarized Carbon Dioxide Concentrator and the spacecraft cabin environment. Principal components of such hardware are a coolant flow diverter valve, a condensing heat exchanger and a liquid-gas separator. These three components were designed, fabricated and tested.

New single cell and subsystem level Test Support Accessories were designed and constructed. The single cell facilities were modifications and refurbishments of previously developed test stands. A new process and cooling Air Supply Unit was constructed for subsystem testing. This closed-loop Air Supply Unit can simulate a spacecraft environment and provides the capability for controlling and monitoring the air temperature, dew point temperature, carbon dioxide partial pressure, oxygen partial pressure and flow rate. This facility is envisioned as a long-term test facility for Electrochemical Depolarized Carbon Dioxide Concentrator Subsystems ranging from a one to six-man capacity.

The technology advancement studies include investigations into three specific areas relating to the Electrochemical Depolarized Carbon Dioxide Concentrator process. These areas were:

1. The influence of the Teflon catalyst binder percentage on performance of the Electrochemical Depolarized Carbon Dioxide Concentrator.

2. The cause of occasionally observed performance deviations associated with maldistributions of carbon dioxide removal rate, water evolution rate and dry bulb temperature variations over the cell electrode surface.

3. The scale-up and fabrication of a cell matrix fabricator.

Based on the results of the technology advancement studies and subsystem development, a new set of performance goals have been adopted. These goals have been defined as performance standards at the subsystem level for future Electrochemical Depolarized Carbon Dioxide Concentrator development. Specifically, a cell voltage of 0.53 V and a carbon dioxide removal efficiency of 82% at a current density of 21.5 mA/cm^2 (20 ASF) have been adopted.

INTRODUCTION

Regenerative processes for the revitalization of spacecraft atmospheres are essential toward making long-termed manned missions in space a reality.[1,2] An important step in this overall revitalization process is the collection and concentration of the metabolically produced carbon dioxide (CO_2) for oxygen (O_2) recovery.

This program continues the development and advancement of an electrochemical CO_2 concentrating process, a technique that allows for the continuous removal of CO_2 from the spacecraft's cabin atmosphere and delivering the CO_2 premixed with hydrogen (H_2) to a CO_2 reduction subsystem for subsequent O_2 recovery.

Background

The Skylab program marked the beginning of the use of regenerative techniques for CO_2 collection by using cyclic absorption/desorption beds containing commercial zeolites. The emerging requirement for obtaining the CO_2 at a partial pressure (pCO_2) below 400 Pa (3 mm Hg) makes the zeolite systems unattractive due to their resulting high weight and volume penalties.[3]

The electrochemical technique of concentrating CO_2 from an air environment has evolved over the past eleven years.[4-9] During this time, the concept has progressed from single cell operation through the fabrication, testing and integration of multi-man, self-contained subsystems for spacecraft application.

The electrochemical removal technique works as follows: CO_2 is continuously removed from a flowing air stream. The removal takes place in an electrochemical module consisting of a series of cells. Each cell consists of two electrodes separated by a matrix containing an aqueous carbonate solution. Plates adjacent to the electrodes provide passageways for distribution of gases and electrical current. Figure 1 shows a functional schematic of the Electrochemical Depolarized CO_2 Concentrator (EDC) cell while Figure 2 details the specific electrochemical and chemical reactions. As shown in Figure 2, the overall reaction is

$$O_2 + 2CO_2 + 2H_2 = 2CO_2 + 2H_2O + \text{electrical energy} + \text{heat}$$

Two moles of CO_2 are theoretically transferred for one mole of O_2 consumed. The observed ratio of CO_2 transferred to O_2 consumed represents the process removal efficiency with 100% efficiency occurring when 2.75 kg (6.05 lb) of CO_2 is removed for each kg (2.2 lb) of O_2 consumed.

Program Objectives

The overall objectives of the present program are (1) to improve the performance of the electrochemical CO_2 removal technique by increasing CO_2 removal efficiencies at pCO_2s below 400 Pa (3 mm Hg), increasing cell power output and broadening the tolerance of electrochemical cells for operation over wide

(1) References cited at the end of this report.

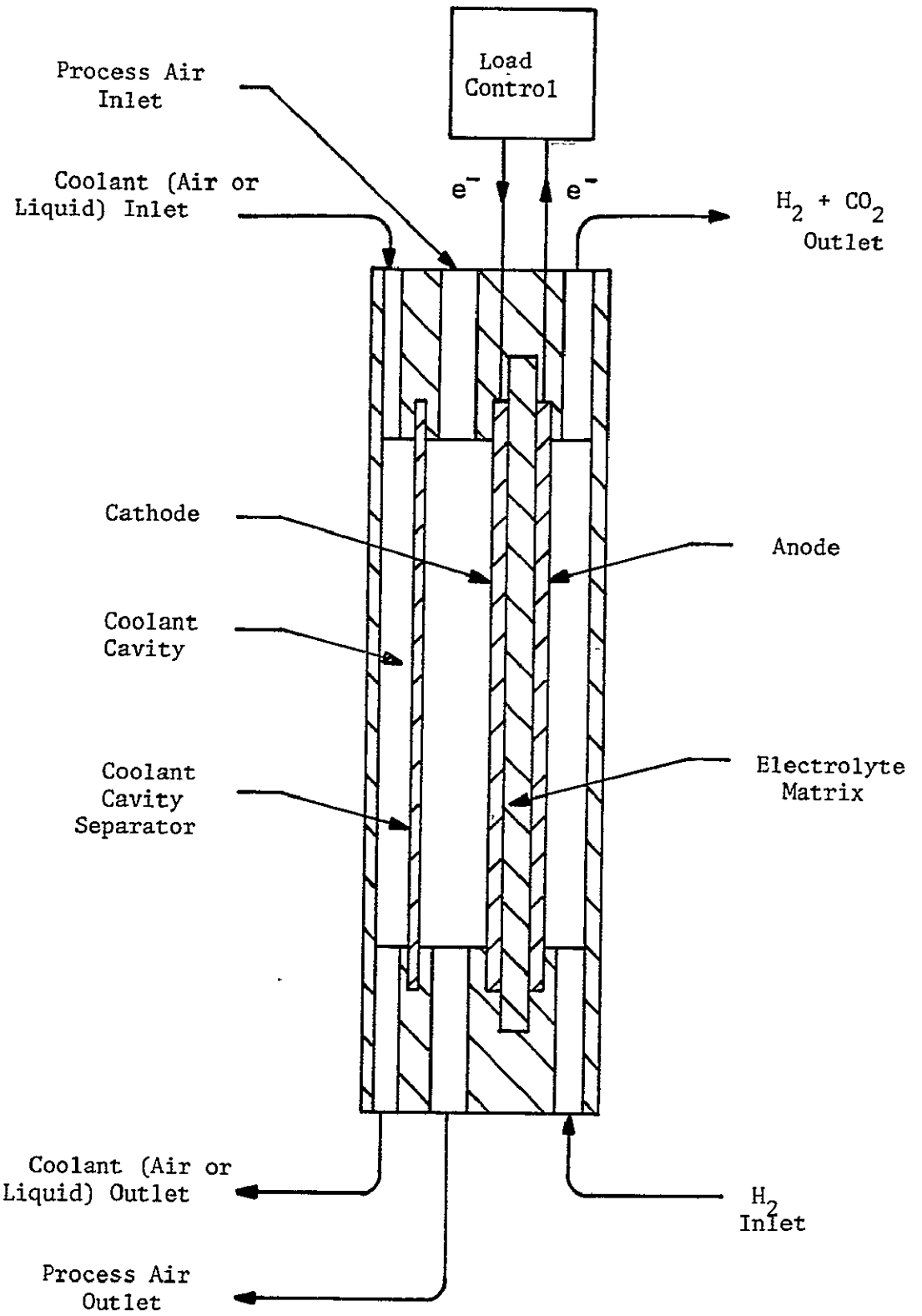

FIGURE 1 EDC CELL FUNCTIONAL SCHEMATIC

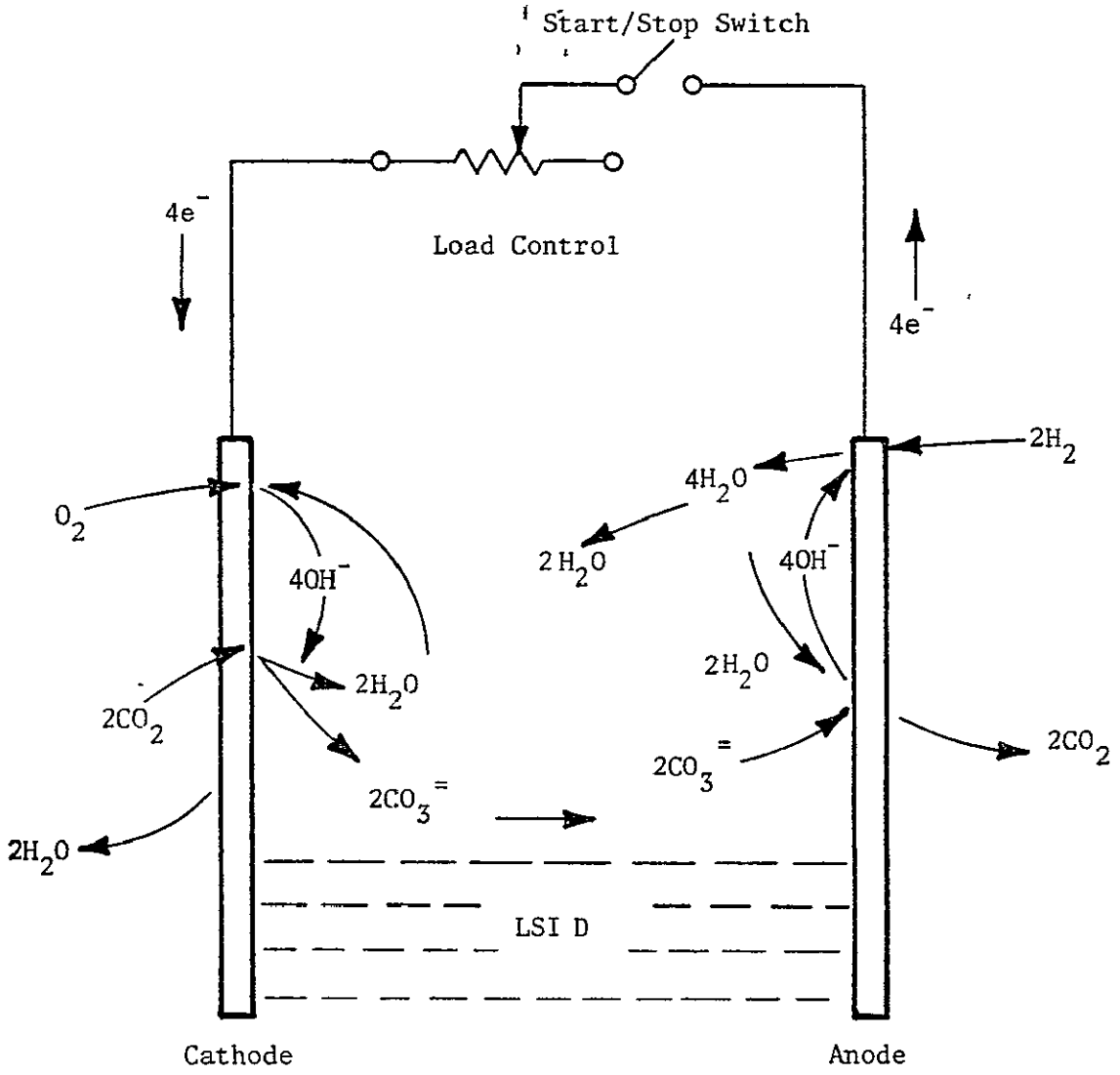

Cathode Reactions:

$O_2 + 2H_2O + 4e^- = 4OH^-$

$4OH^- + 2CO_2 = 2H_2O + 2CO_3^=$

Anode Reactions:

$2H_2 + 4OH^- = 4H_2O + 4e^-$

$2CO_3^= + 2H_2O = 4OH^- + 2CO_2$

Overall Reaction:

$O_2 + 2CO_2 + 2H_2 = 2CO_2 + 2H_2O$ + Electrical Energy + Heat

FIGURE 2 EDC ELECTROCHEMICAL AND CHEMICAL REACTIONS

ranges of cabin relative humidity (RH); (2) design, fabricate and assemble development hardware to evolve the electrochemical concentrating technology from the existing level to an advanced level able to simultaneously meet the CO_2 and water removal needs of a spacecraft Air Revitalization System (ARS); (3) develop and incorporate into the subsystem hardware components and concepts that allow for the efficient integration of the electrochemical technique with other subsystems to form a spacecraft ARS.

Program Organization

To meet the above objectives, the program has been divided into five tasks plus the documentation and program management functions. The five tasks are:

1.0 Design, fabricate and assemble development hardware to evolve the EDC subsystem's technology from the existing level to an advanced level capable of efficiently removing CO_2 from a spacecraft's atmosphere and able to be integrated with other Environmental Control/ Life Support System (EC/LSS) subsystems to form a spacecraft ARS.

2.0 Design, develop, fabricate, assemble, functionally checkout and calibrate Test Support Accessories (TSA) to be compatible with the test objectives of the EDC related hardware (Task 4.0) and the supporting research and technology testing (Task 5.0).

3.0 Establish, implement and maintain a mini-Product Assurance Program through all phases of contractual performance, including designing, fabricating, purchasing, assembling, testing, packaging and shipping consistent with a program in the early stages of development.

4.0 Perform a variety of subsystem and integrated subsystem testing required to demonstrate readiness of the EDC concept.

5.0 Complete essential and desirable supporting research and development efforts to further expand the technology base associated with spacecraft EDC. Special emphasis shall be placed on the development of the heart of an electrochemical cell, the electrodes, the electrolyte retaining matrix and the electrolyte.

Report Organization

This Annual Report covers the work performed from the start of the program, February, 1975, through March, 1977. The following four sections present the technical results grouped according to (1) Subsystem Developments, (2) Component Developments, (3) TSA Developments and (4) Technology Advancement Studies. These sections are followed by Conclusions and Recommendations based on the work performed.

SUBSYSTEM DEVELOPMENTS

The subsystem development activities performed as part of this program included (1) continuing advancement of liquid-cooled EDCs and (2) providing support and hardware to integrated subsystem test and development programs.

Liquid-Cooled EDC

Activities completed under previous EDC development programs had shown that liquid-cooled EDC cells exhibited substantially higher CO_2 removal efficiencies than air-cooled cells, especially at low pCO_2 levels.[10] The result of such testing is demonstrated in Figure 3. The CO_2 removal efficiency is plotted versus process air inlet pCO_2 for a liquid-cooled single cell and compared to a least squares fit of previous EDC performance data. The testing was performed with a modified old style 2.3 dm^2 (0.25 ft^2) cell.

Subsequent development activities resulted in the design and fabrication of a lightweight, advanced EDC cell frame capable of being injection molded with provisions for either internal air cooling or internal liquid cooling. As part of this program, a one-man capacity, liquid-cooled module was fabricated using the advanced liquid-cooled cells and tested as part of a one-man laboratory breadboard Sabatier-based O_2 reclamation system (LBS-S/ORS-1(L)). To test the one-man, liquid-cooled advanced module, the hardware developed for a one-man, self-contained CO_2 concentrating subsystem (CX-1)[5] was refurbished and modified. Similarly, the TSA previously used with the CX-1 was modified to support the projected liquid-cooled module testing.

Past liquid-cooled performance data had indicated that a five-cell module operating at 30 mA/cm^2 (28 ASF) could remove the 1 kg/d (2.2 lb/d) CO_2 metabolically generated by one man.[10]

Five advanced liquid-cooled cell frames were fabricated. The frames used the advanced lightweight plated anode current collector concept. Figure 4 shows a functional schematic of internally liquid-cooled advanced cell frames. Figures 5 and 6 show the liquid-cooled cell frame and the parts that make up an advanced liquid-cooled cell, respectively. The five cells were assembled using plexiglass endplates. Following assembly, the module was charged with 61.5% cesium carbonate (Cs_2CO_3) electrolyte.

Following refurbishment and modification to the CX-1 and its TSA, the one-man capacity module was integrated with the test system and shakedown and checkout testing was successfully completed. The major modifications included upgrading of the system's current capability to allow operation of the larger (4.6 dm^2 (0.5 ft^2) versus 2.3 dm^2 (0.25 ft^2)) advanced cells at elevated current densities. Also, provisions for liquid cooling, including feedback controlled temperatures, were added to the system and TSA. Endurance testing of the one-man module was completed as part of integrated testing with an O_2 Generation Subsystem (OGS) and a Sabatier-based CO_2 Reduction Subsystem (SCRS) described below.

Subsystem Integrations

Subsystem integration support activities were performed at two levels:

1. To test a liquid-cooled EDC as part of a LBS-S/ORS-1(L);

2. To test an air-cooled EDC, including the process air humidity control subsystem, as part of a laboratory breadboard Bosch-based O_2 reclamation system at the four-man level (LBS-B/ORS-4(A)).

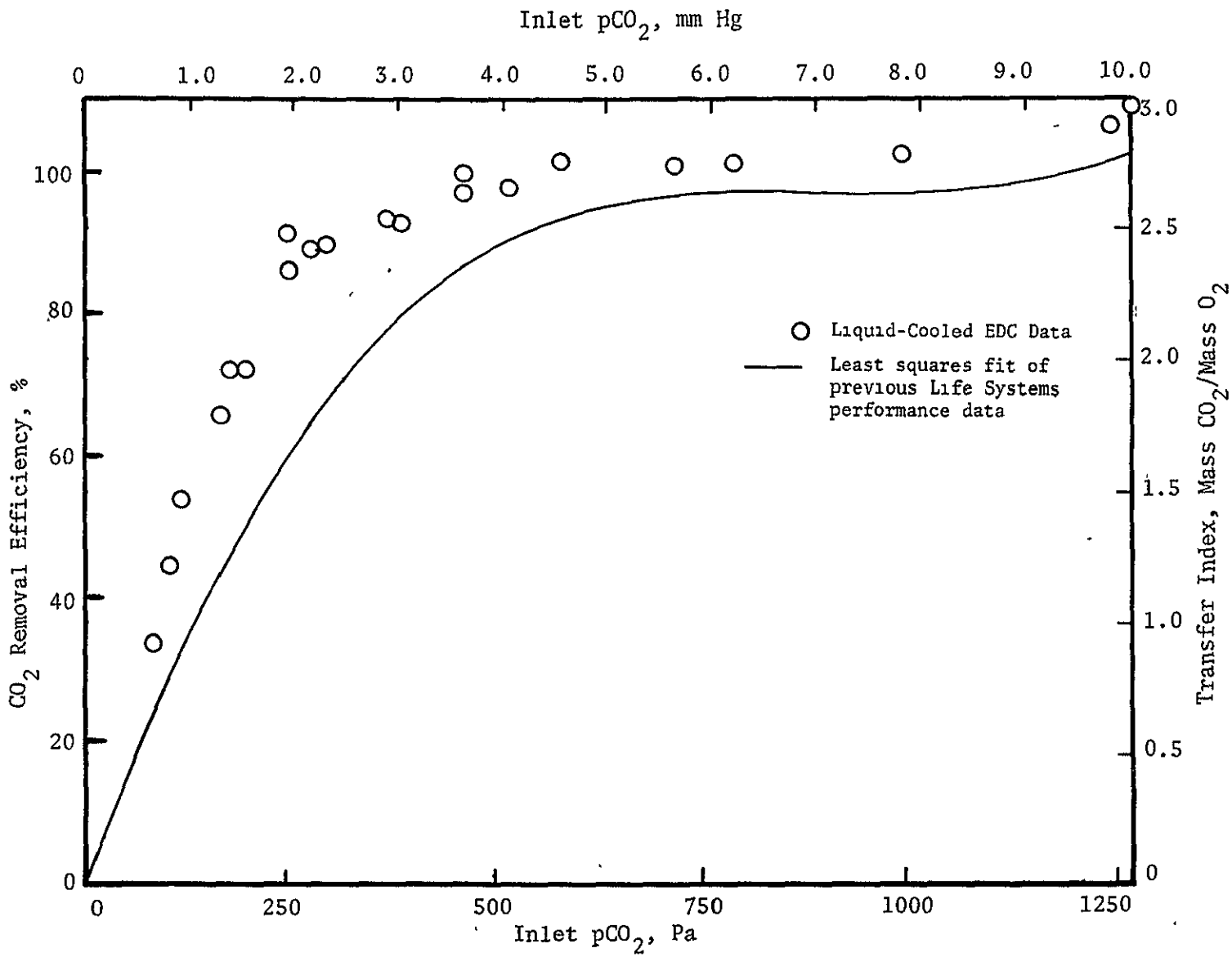

FIGURE 3 LIQUID-COOLED EDC PERFORMANCE AS A FUNCTION OF AIR INLET pCO_2

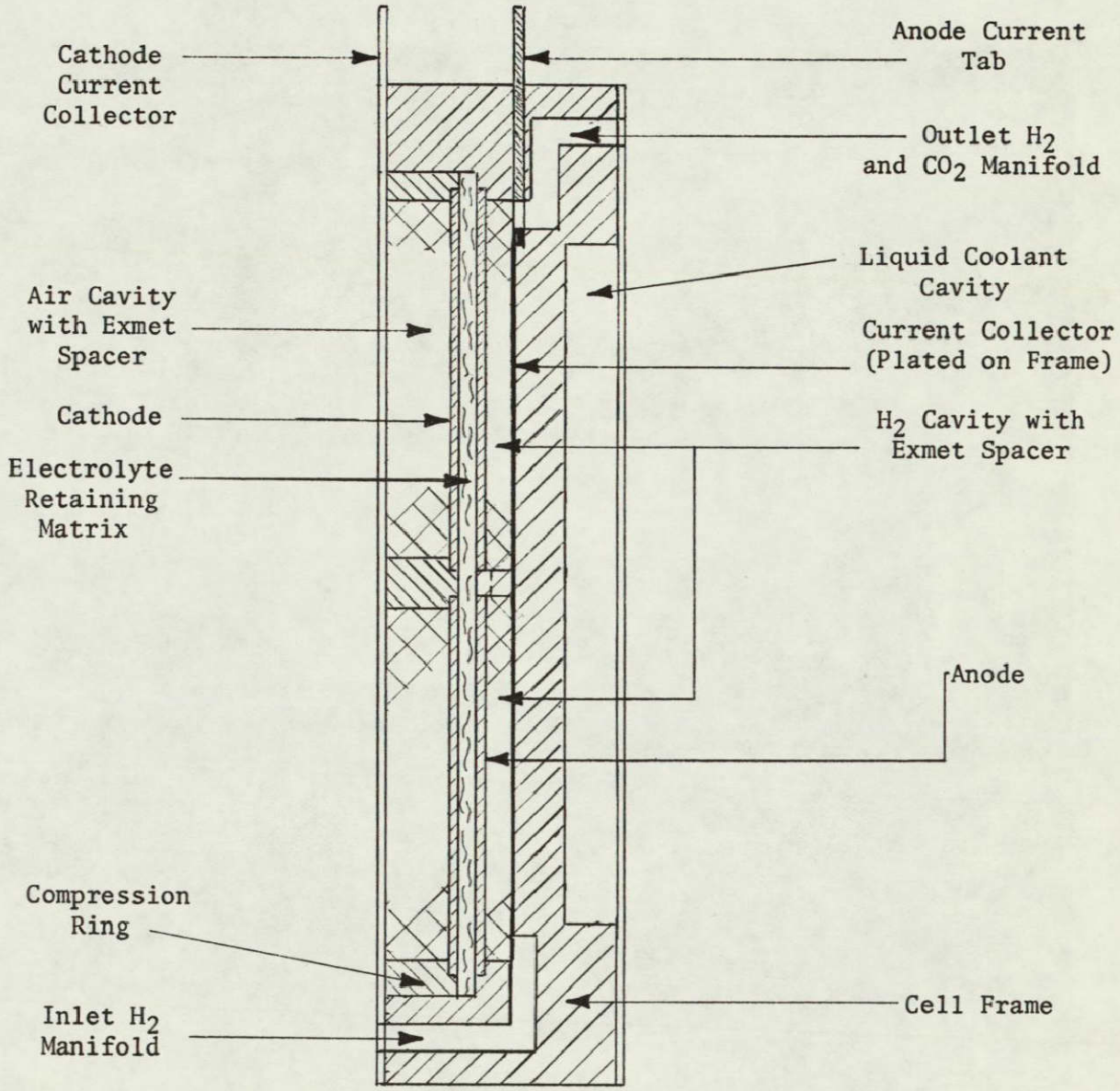

FIGURE 4 ADVANCED LIQUID COOLED EDC CELL FUNCTIONAL SCHEMATIC

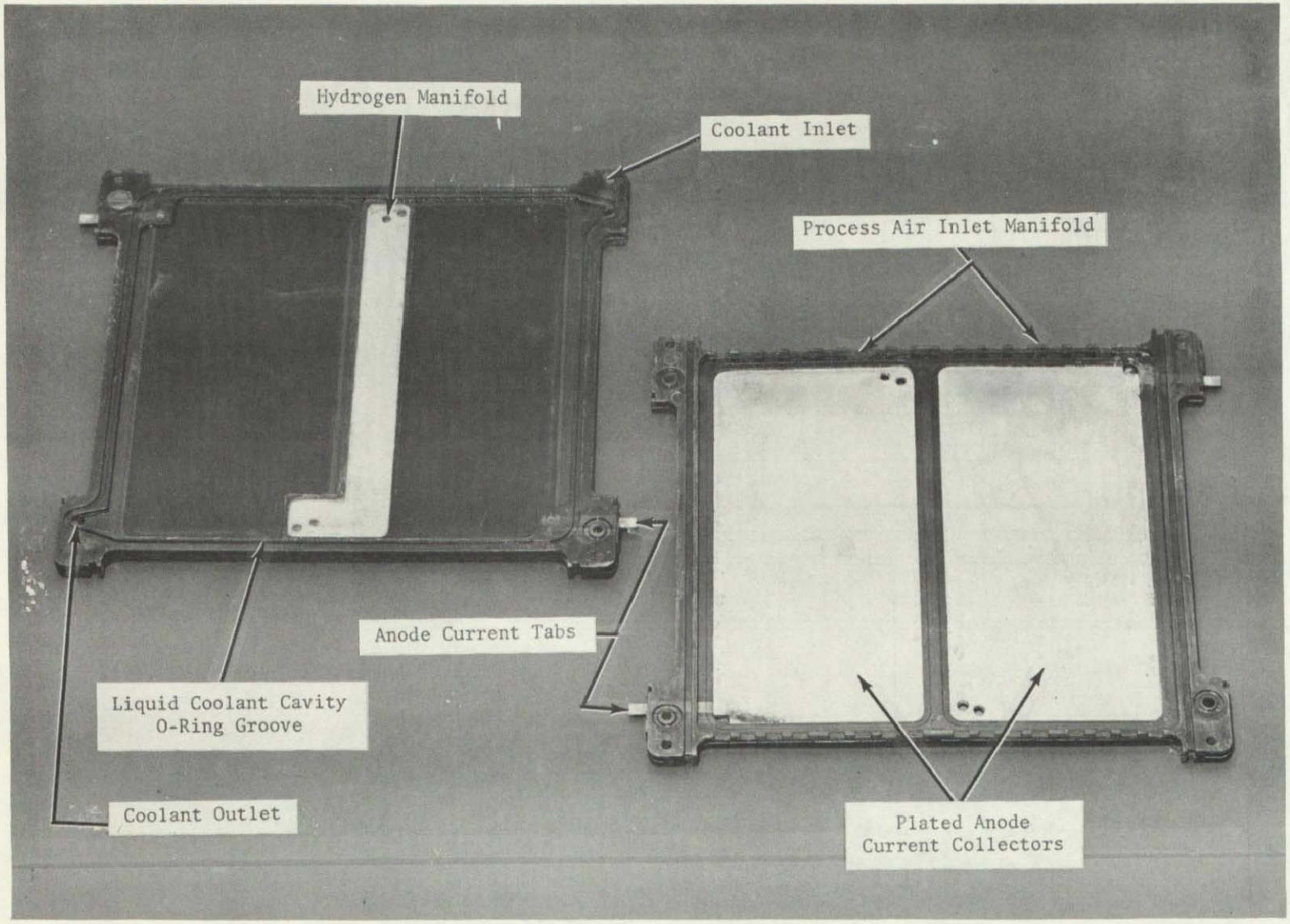

FIGURE 5 ADVANCED EDC CELL FRAME FOR LIQUID COOLING

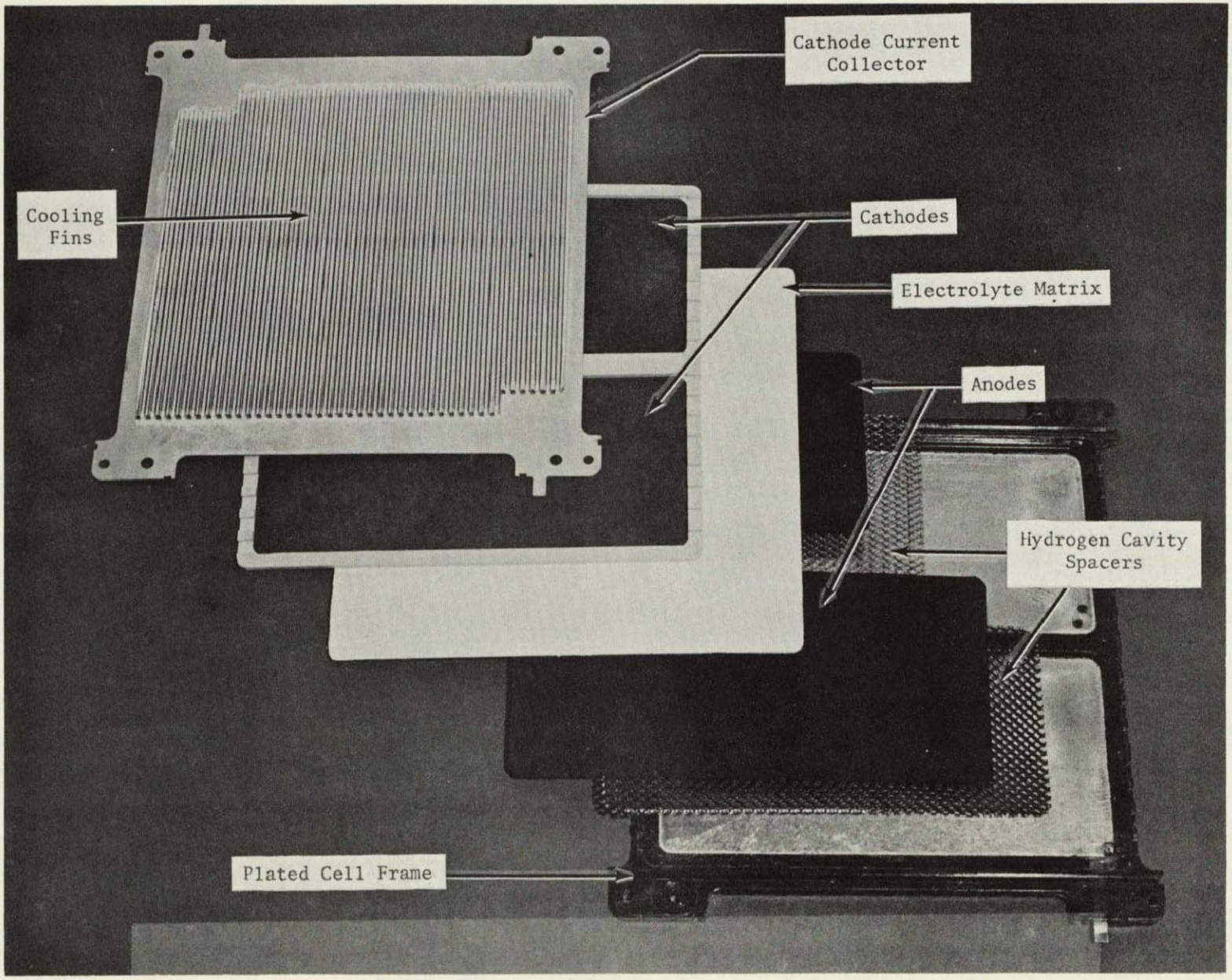

FIGURE 6 ADVANCED EDC LIQUID-COOLED CELL PARTS

These integration support activities were performed to develop EDCs, based on both the liquid-cooled and air-cooled concept, that are capable of being integrated with other EC/LSS subsystems to form spacecraft ORS or total ARS.

Benefits of testing EC/LSS subsystems as part of an ORS or ARS are:

- Verification of the integratability of a specific subsystem, i.e., accumulation and generation of integration technology
- Reduction in TSA since other subsystems supply required fluid interfaces
- Elimination of commonality components
- Reduction in test program costs

One-Man Laboratory Breadboard

The one-man capacity, liquid-cooled EDC was integrated with an OGS and an S-CRS to form a LBS-S/ORS-1(L) and was tested for a 30-day period. The overall objectives of the test were to:

- Demonstrate long-term, multi-cell, liquid-cooled EDC operation using advanced cell hardware
- Test the EDC with OGS generated H_2
- Test the Contractor-developed Sabatier reactor with EDC exhaust gas, i.e., H_2, CO_2 and water vapor
- Expand integration technology by operating three subsystems as one ORS

Figure 7 is a block diagram of the one-man ORS. As Figure 7 shows, the integrated system had a capability to vary the amount of H_2 entering the EDC or the Sabatier reactor by supplying an external H_2 source. This could simulate eventual integration with the N_2 Supply Subsystem (NSS) based on hydrazine (N_2H_4) technology.

Figures 8, 9 and 10 are photographs of the EDC, OGS and Sabatier reactor used as part of the one-man ORS. The Sabatier reactor was developed and fabricated as part of a Contractor-funded activity but was tested as part of the present program. Figure 11 shows the integrated one-man ORS test facilities, including TSA. Following individual subsystem shakedown testing, a 30-day integrated endurance test was performed. Prior to test initiation, baseline operating conditions for the integrated system were established. These conditions are listed in Table 1. The endurance test was performed with maintaining the baseline conditions at constant values.

The performance of the one-man, liquid-cooled EDC and the S-CRS for the 30 days of testing is shown in Figure 12. Of special interest is the high cell voltage of 0.4 V per cell for the EDC and the high average transfer efficiency of 76% (TI of 2.1) for the duration of the test considering that the advanced module is

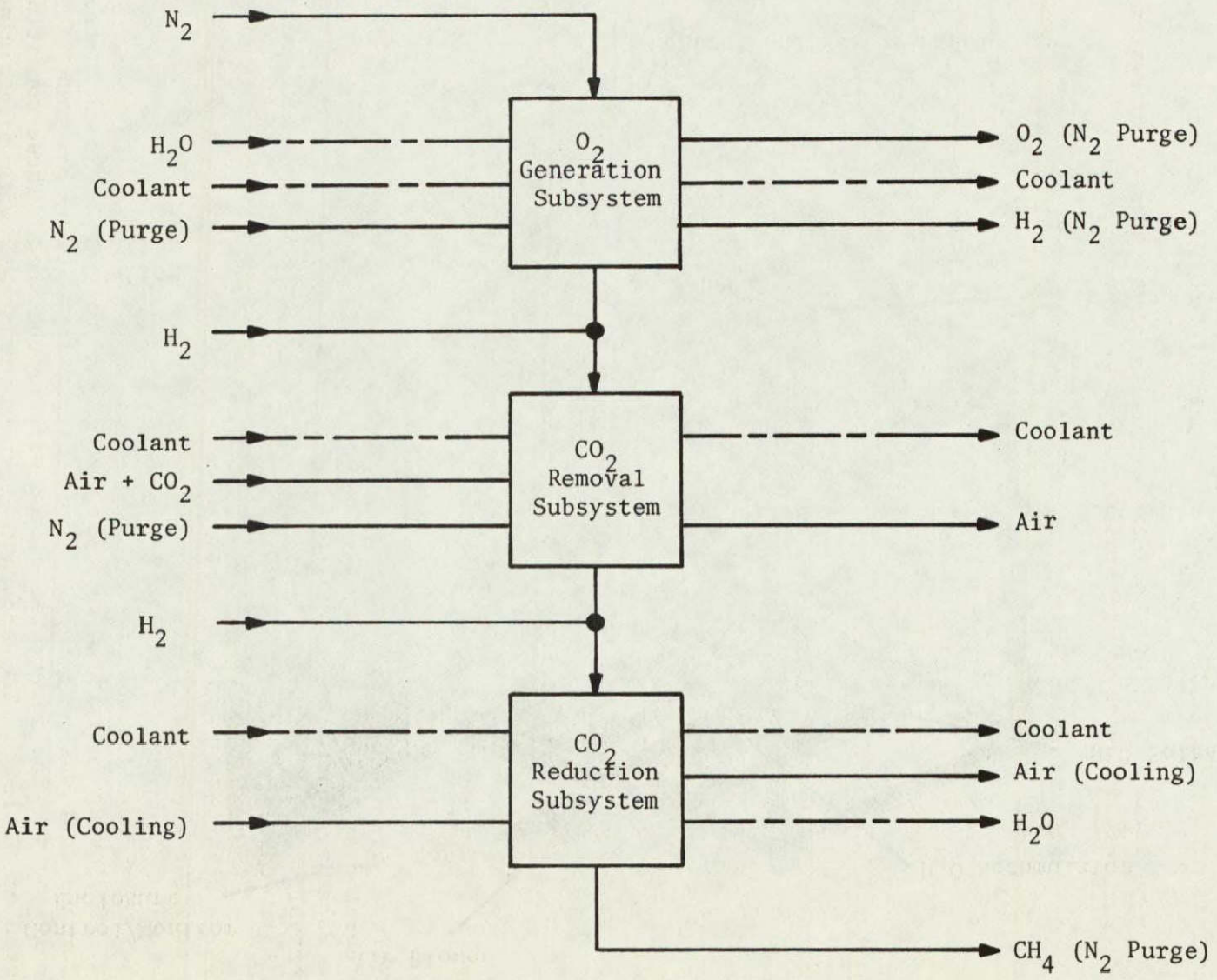

FIGURE 7 ONE-MAN OXYGEN RECOVERY SYSTEM BLOCK DIAGRAM

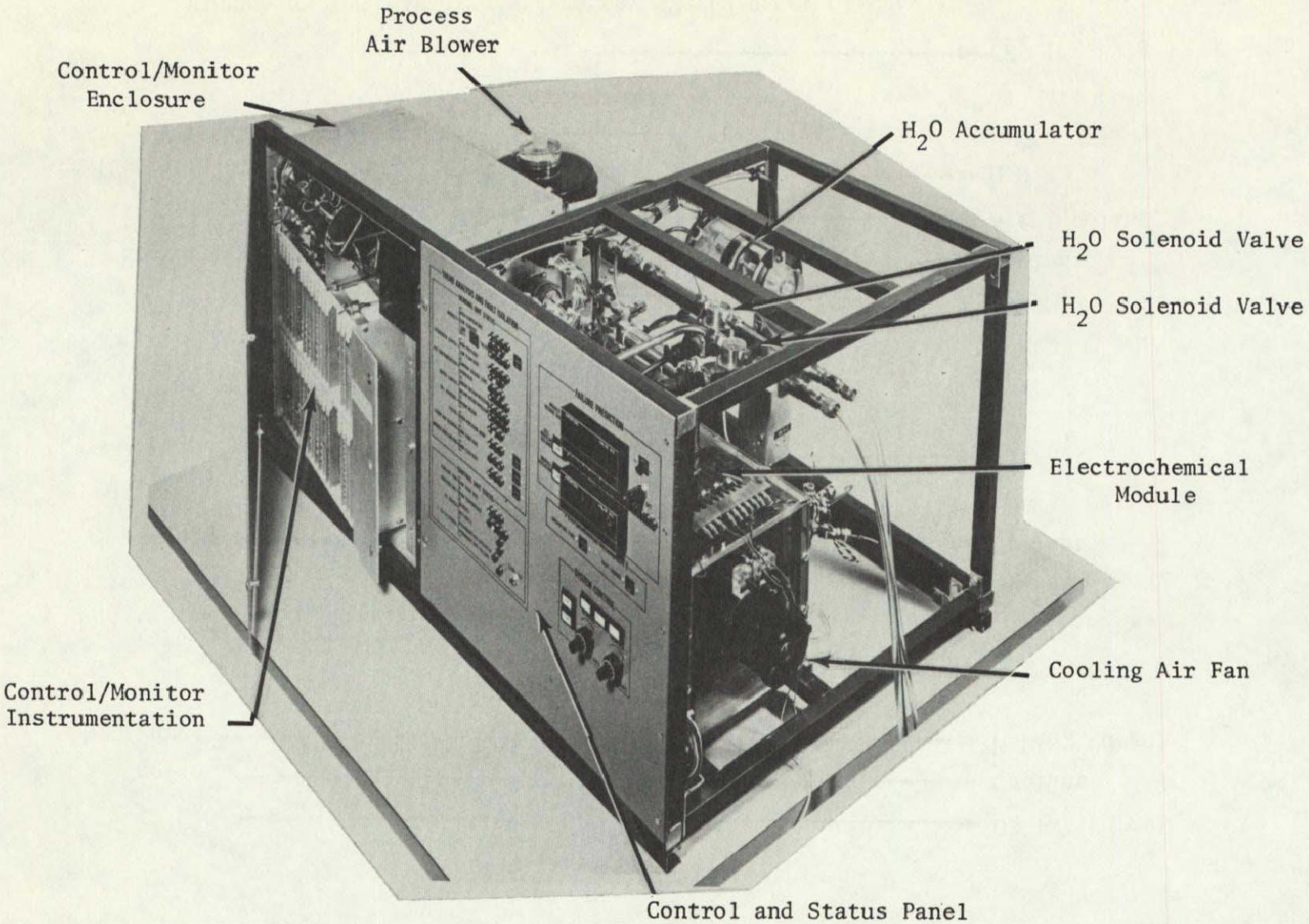

FIGURE 8 ONE-MAN ELECTROCHEMICAL DEPOLARIZED CO_2 CONCENTRATOR

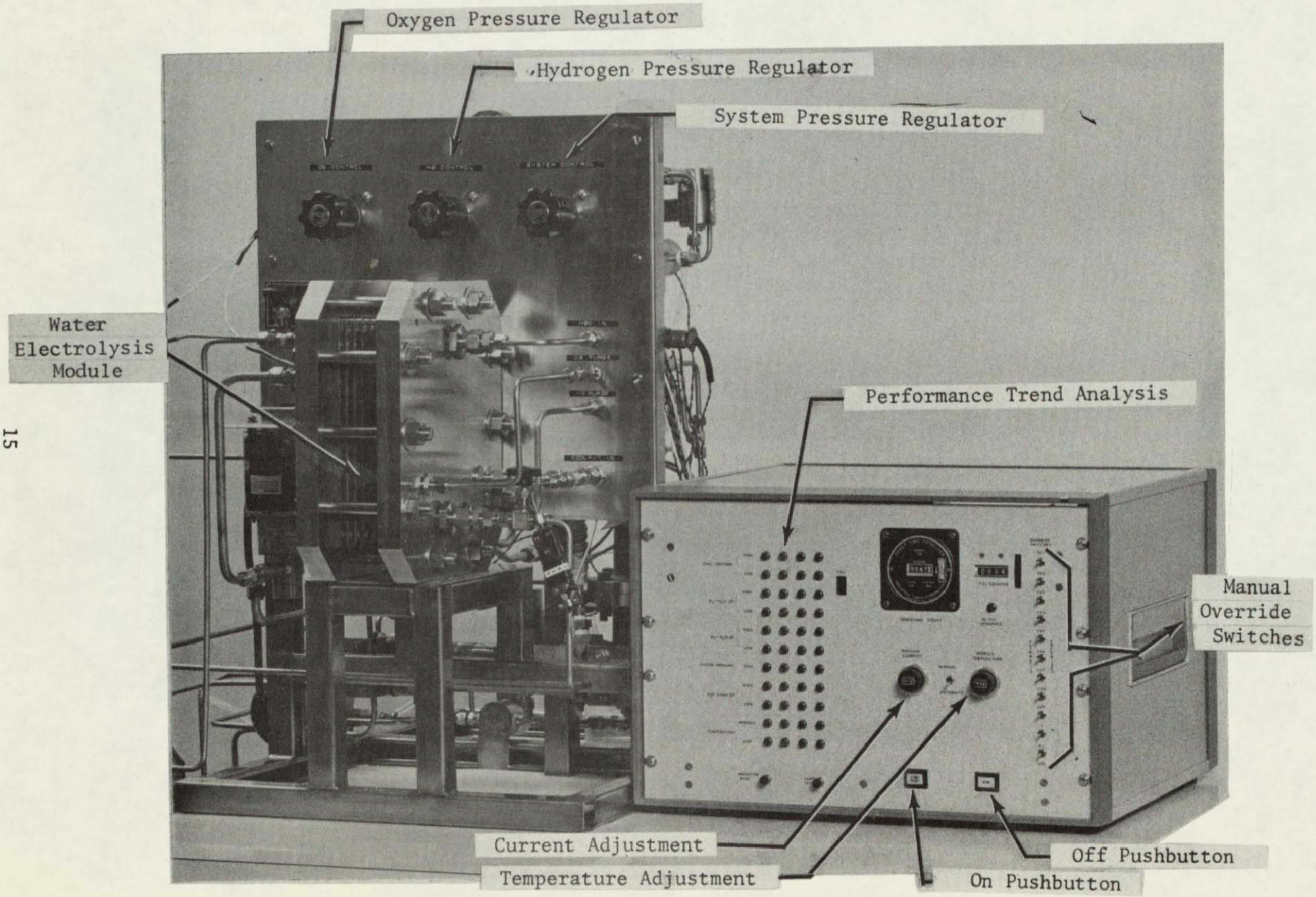

FIGURE 9 ONE-MAN OXYGEN GENERATION SYSTEM

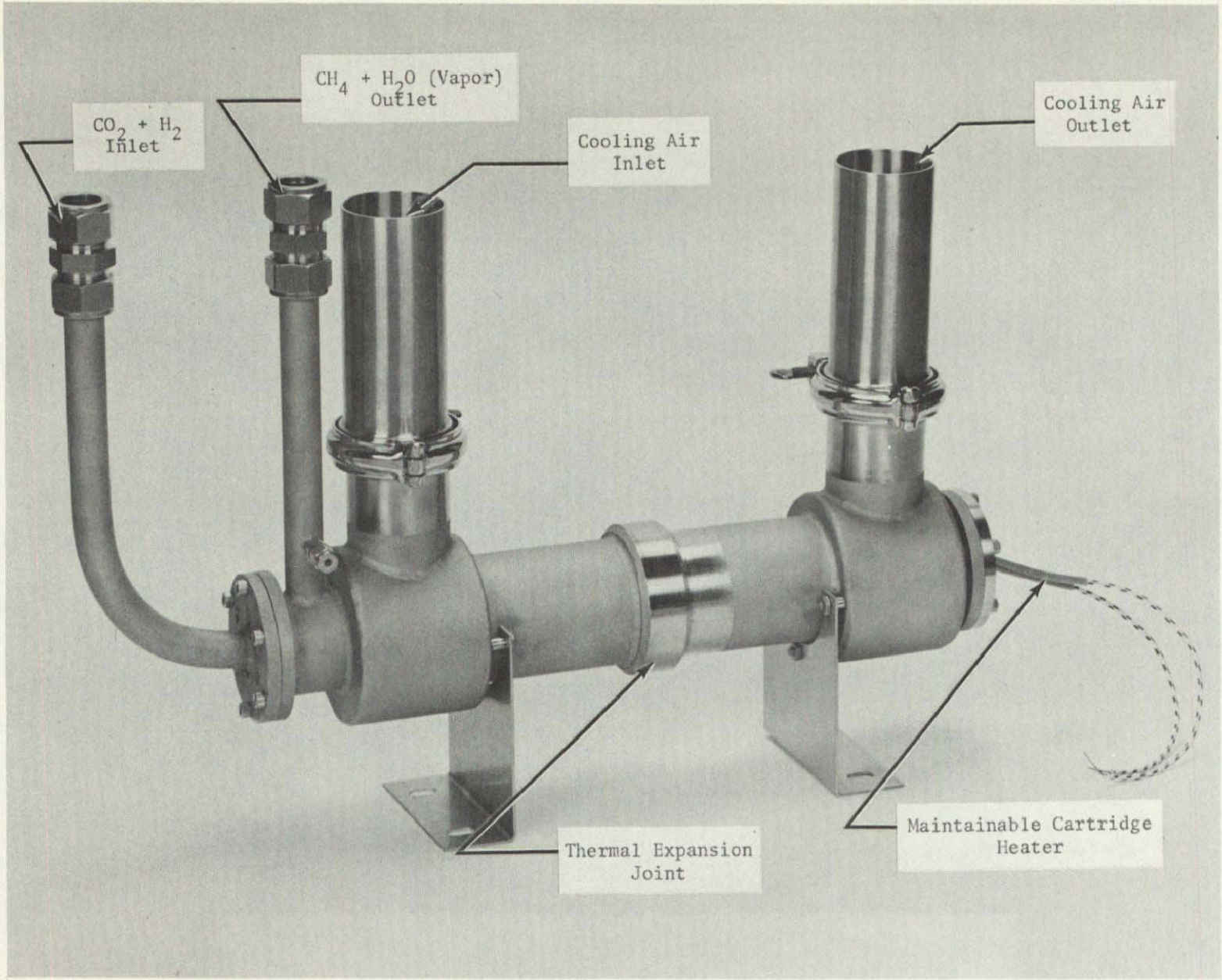

FIGURE 10 ONE- TO THREE-MAN SABATIER REACTOR

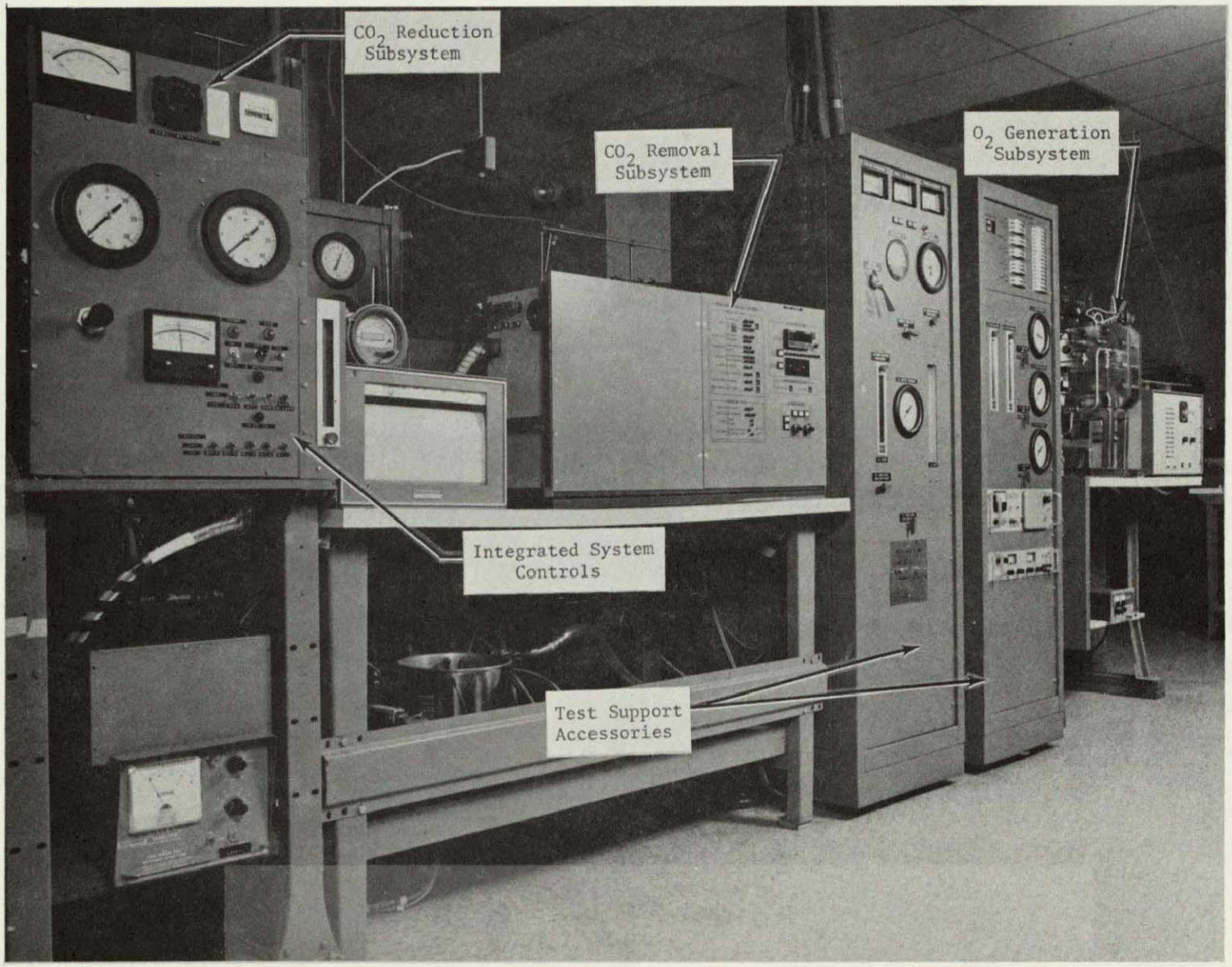

FIGURE 11 ONE-MAN LABORATORY SYSTEM TEST FACILITY

TABLE 1 BASELINE OPERATING CONDITIONS FOR THE LBS-S/ORS-1(L)

Process Air Inlet	
pCO_2, Pa (mm Hg)	400 (3.0)
Air Flow Rate, dm^3/min (scfm)	226.5 (8.0)
Dew Point Temperature, K (F)	286 to 289 (56 to 60)
Dry Bulb Temperature, K (F)	291 to 294 (65 to 70)
Relative Humidity, %	61 to 84
EDC Module	
Number of Cells	5
Current, A	13.7
Current Density, mA/cm^2 (ASF)	30.1 (28)
Temperature, K (F)	296 to 298 (73 to 77)
Pressure, kPa (psia)	101 (14.7)
Cell Voltage, V	0.3
CO_2 Removal Efficiency, %	74
Power Generated, W	20.6
Heat Generated, W	65.1
Water Electrolysis Module	
Number of Cells	6
Cell Current, A	19.4
Cell Current Density, mA/cm^2 (ASF)	208.7 (194)
Temperature, K (F)	333 to 339 (140 to 150)
Pressure, kPa (psia)	965 (140)
Cell Voltage, V	1.60
Power Required, W	186.2
Heat Generated, W	14.0
Sabatier Reactor	
Temperature, K (F)	644 (700)
Pressure, kPa (psia)	108 (15.7)
CO_2 Reduction Efficiency, %	68
H_2 Conversion Efficiency, %	96

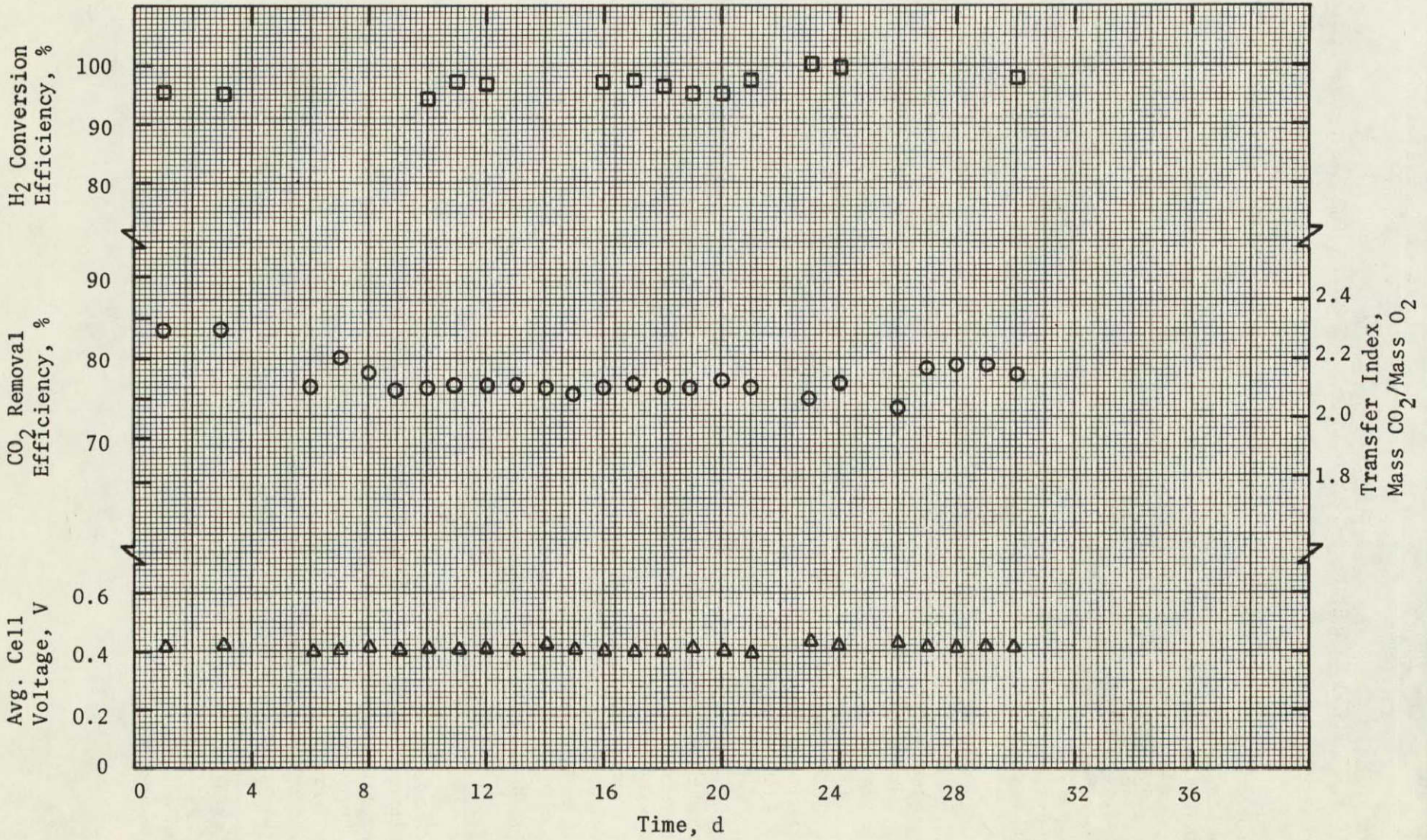

FIGURE 12 EDC AND SABATIER PERFORMANCES FOR 30-DAY INTEGRATED ENDURANCE TEST

operated at a current density of 30 mA/cm^2 (28 ASF). As shown, the H_2 conversion efficiency of the Sabatier reactor averaged approximately 97% throughout the total test time.

In addition to the performance characteristics obtained from the testing, significant contributions to the operation of integrated systems were established in the areas of startup sequence, shutdown sequence, common system purge and subsystem performance monitoring.

Four-Man Laboratory Breadboard

A four-man capacity, air-cooled EDC (CXA-4(A)) was modified and refurbished to support testing of a LBS-B/ORS-4(A) being tested under a separate NASA-funded program.[11] Figure 13 is a block diagram showing the closed O_2 loop system with an integrated EDC, Bosch Reduction Subsystem (BRS) and OGS.

A previously developed six-man capacity, self-contained EDC[6] was refurbished and modified to form the CXA-4(A). Only three of the six one-man design capacity modules were used to provide the CO_2 removal capacity for four men, e.g., 4 kg CO_2/d (8.8 lb CO_2/d). To achieve the extra CO_2 removal rate, the modules are to be operated at the higher than design current density (26.9 versus 22.6 mA/cm^2 (25 versus 21 ASF)). A block diagram of the CXA-4(A) is shown in Figure 14. This EDC was based on the A-level of technology, i.e., technology developed prior to the advanced lightweight module development. The A-level technology definition for the CXA-4(A) modules is shown in Table 2.

In a spacecraft environment, CO_2 removal subsystem functioning as part of an overall ARS will receive its process and cooling air from a humidity control subsystem. To simulate this operating condition, an EDC process air and humidity control subsystem at the breadboard level was designed and fabricated. A schematic of this subsystem is shown in Figure 15. The major components include a condensing heat exchanger with water air collection section, a vortex type liquid/gas separator, two blowers and a coolant flow control valve. The subsystem was sized to supply process and cooling air to EDCs ranging from one to six man capacity (up to 14 m^3/min (500 cfm)).

The coolant flow diverter valve was designed, fabricated and tested as part of this program and is discussed in the following section. The condensing heat exchanger was constructed of a stainless steel housing with stainless steel coolant tubes having copper fins. Copper was selected over aluminum to enhance long life corrosion resistance in the high pCO_2 (acidic) environment. A vortex separator, fabricated from acrylic plastic to allow visual observation was integrated with the subsystem. Blowers, valves, filters and pumps were off-the-shelf components. Figures 16 and 17 are photographs of the condensing heat exchanger and vortex-type liquid/gas separator, respectively.

Integrated checkout and shakedown testing of the CXA-4(A) and the EDC process air humidity control subsystem as part of the integrated LBS-B/ORS-4(A) has been successfully completed. Integrated endurance testing for up to 30 days of operation is scheduled for the next reporting period.

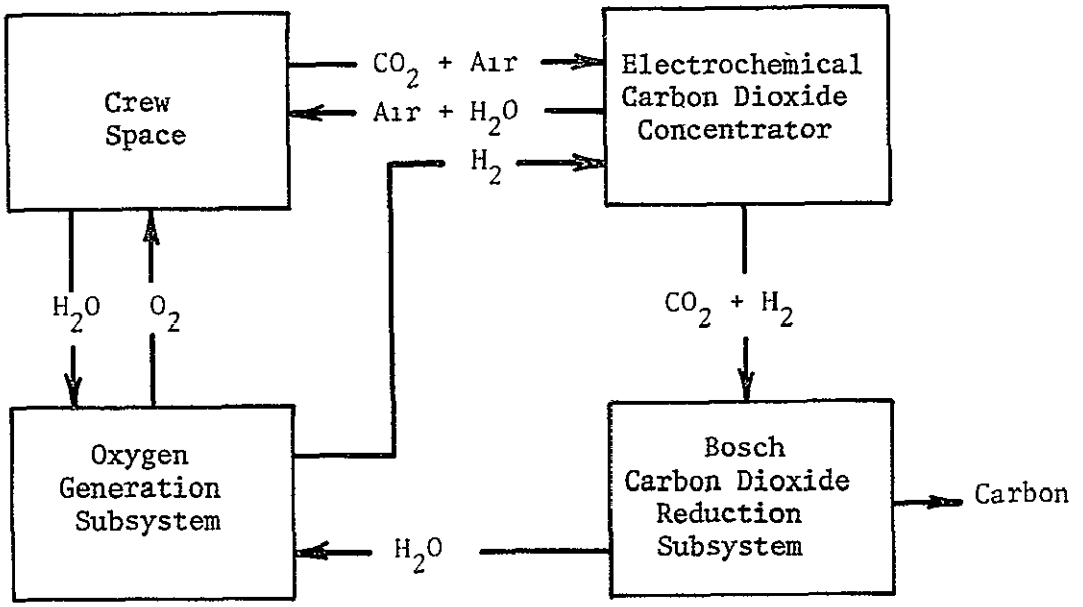

FIGURE 13 CLOSED OXYGEN LOOP WITH INTEGRATED EDC/BRS/OGS

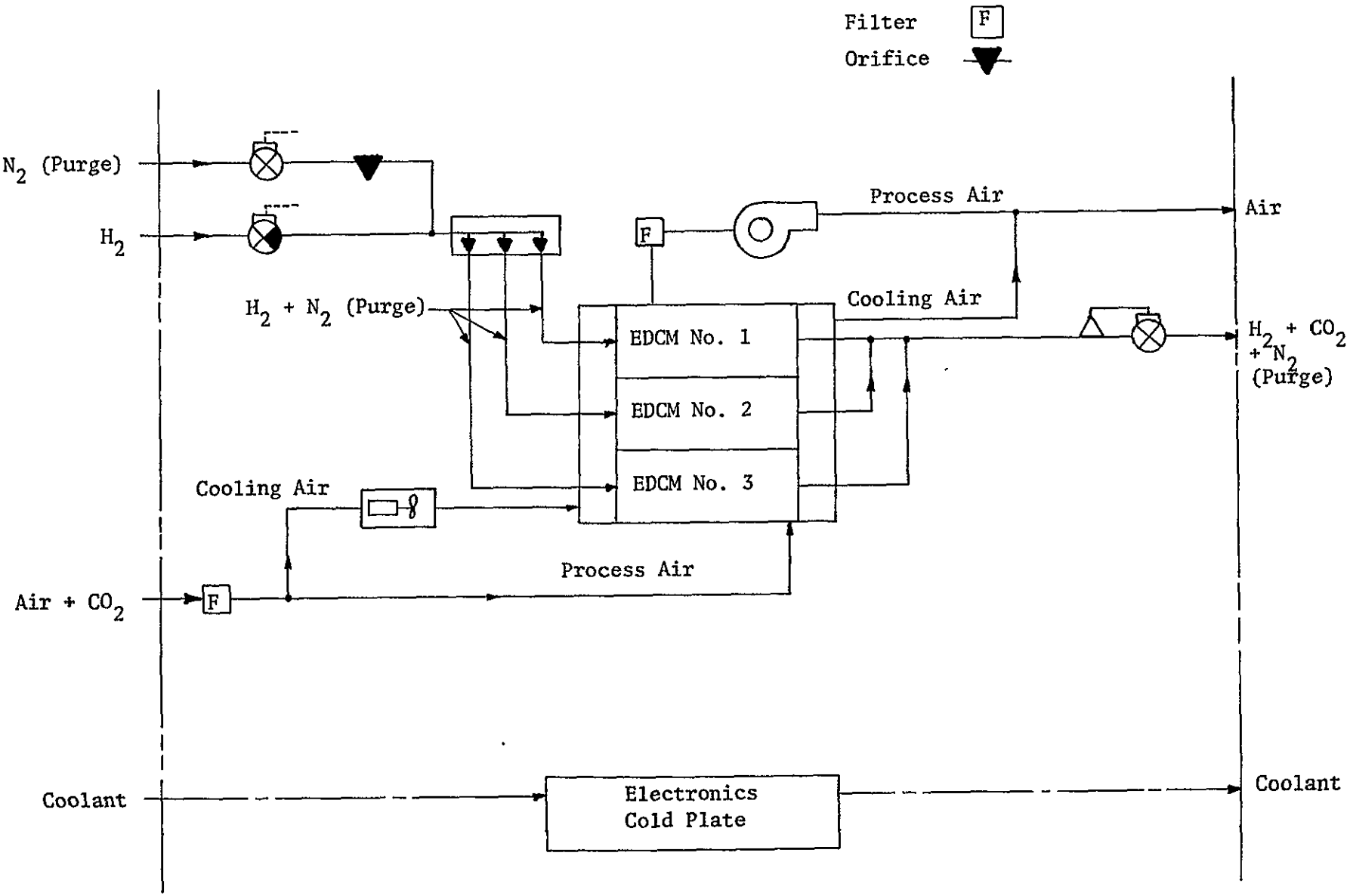

FIGURE 14 CXA-4(A) BLOCK DIAGRAM

TABLE 2 A-LEVEL TECHNOLOGY DEFINITION
FOR CXA-4(A) MODULES

Module Subelement	Subelement Designation
Anode	BE1
Electrolyte	LSI-D
Matrix	BM-2
Cathode	BE1
Bipolar Plate	Au/Ni
Cell Frame	Polysulfone
Endplate	Stainless Steel
O-Ring/Gasket	Ethylene Propylene

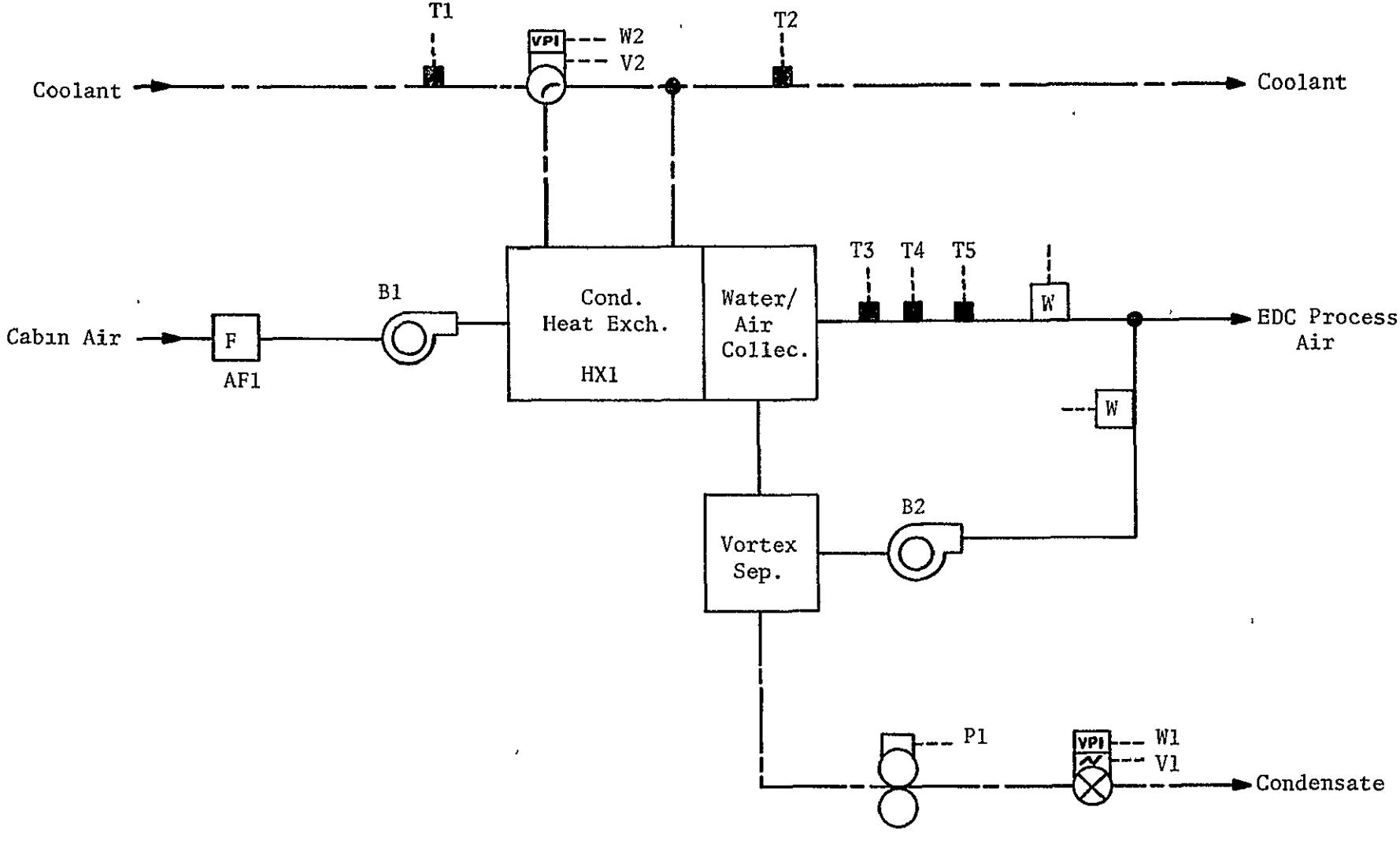

FIGURE 15 EDC PROCESS AIR AND HUMIDITY CONTROL SUBSYSTEM SCHEMATIC

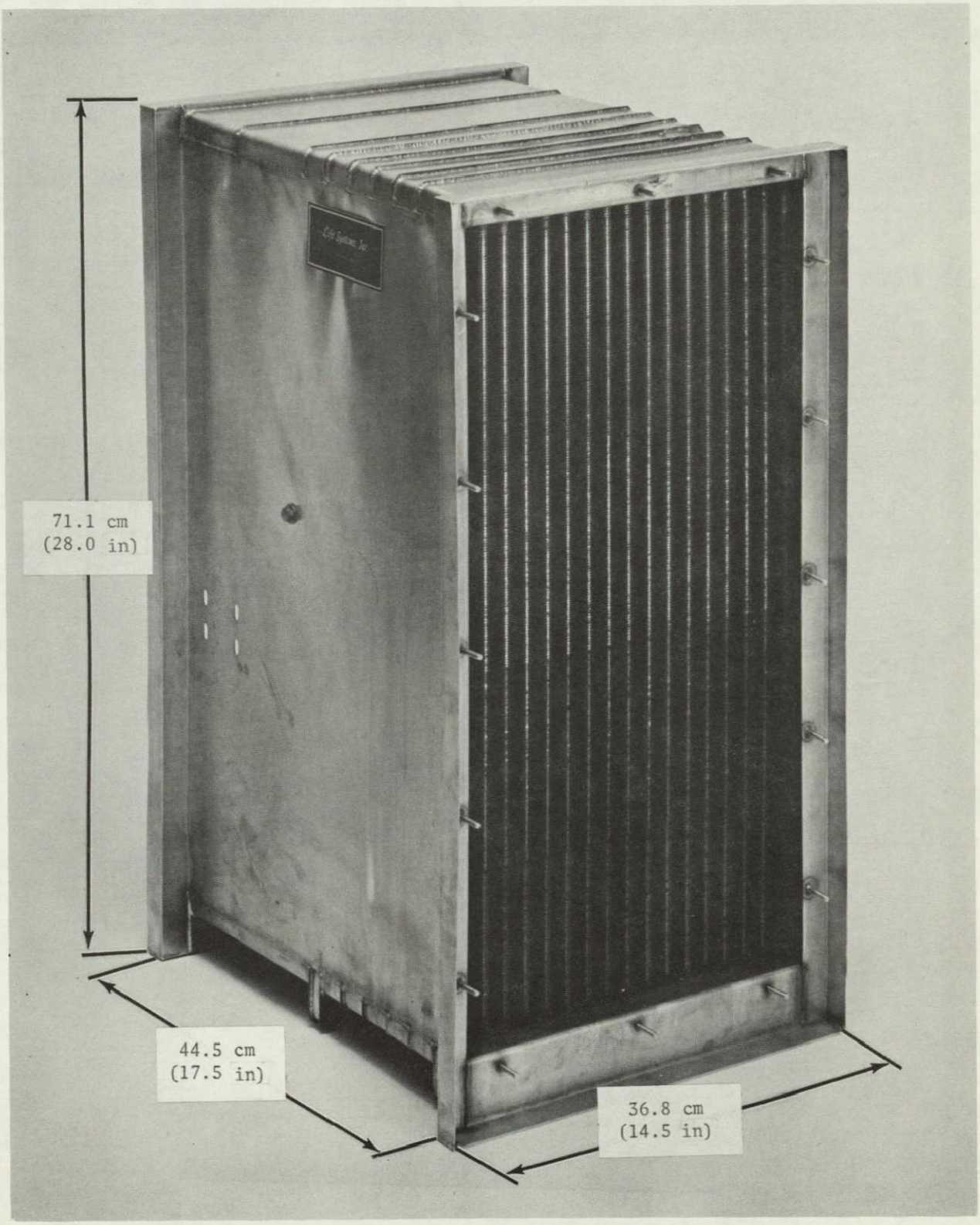

FIGURE 16 CONDENSING HEAT EXCHANGER

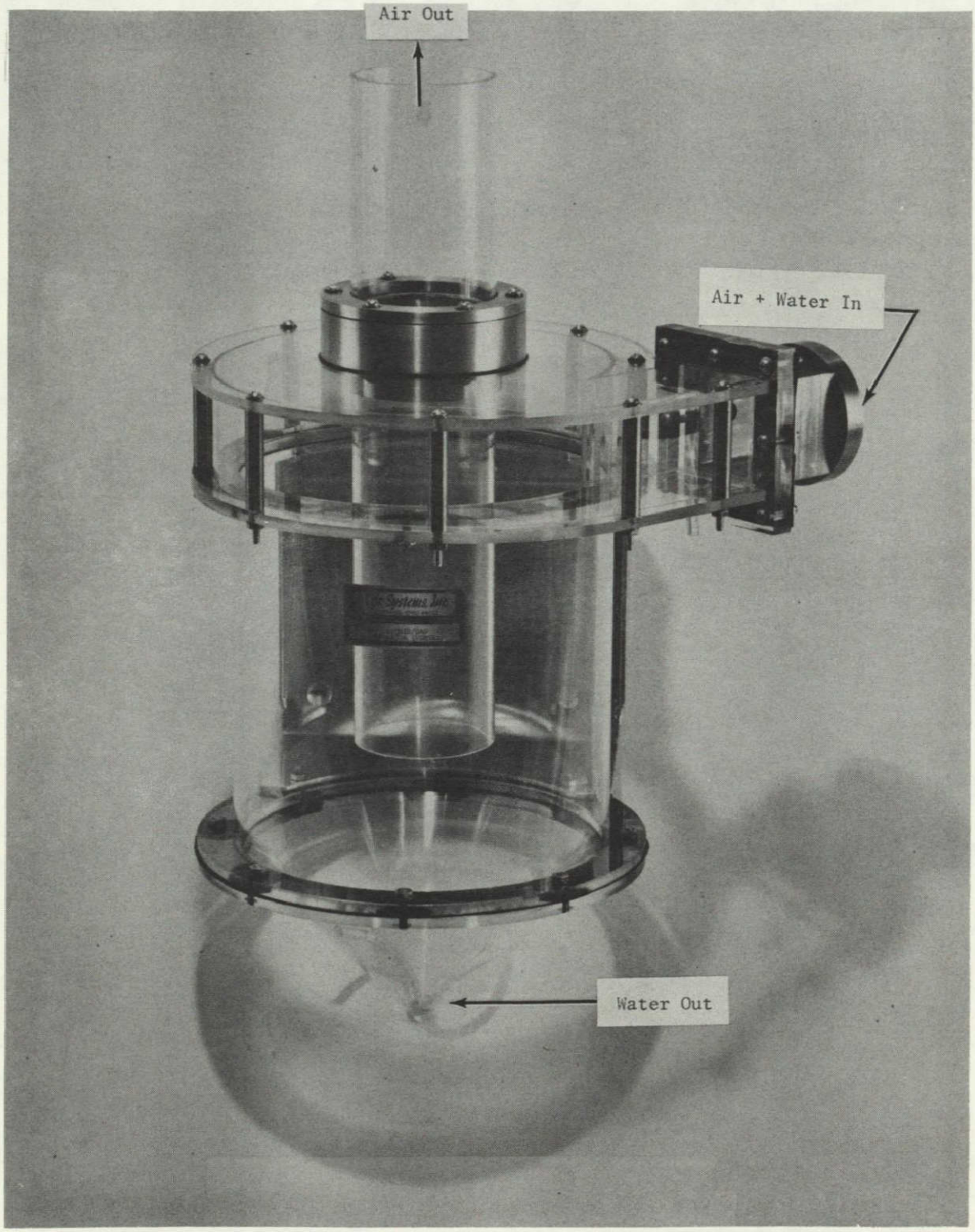

FIGURE 17 VORTEX LIQUID/GAS SEPARATOR

COMPONENT DEVELOPMENTS

Several hardware components were developed as part of the humidity control subsystem for an experimental one-man metabolic capacity unit based on a liquid-cooled EDC. The three principal components of this subsystem are a coolant flow diverter valve, a condensing heat exchanger and a liquid/gas separator. Figure 18 shows these components in the overall schematic of an EDC process air conditioning and humidity control subsystem. The function of this subsystem is to control dew point of the cabin air exiting from the heat exchanger. The diverter valve adjusts the flow of constant temperature coolant to the heat exchanger. The water that is condensed out of the cabin air is removed from the heat exchanger by a separate blower through the liquid/gas separator. Following separation, the collected condensate is pumped to a storage tank.

Coolant Flow Diverter Valve

The development of a condensing heat exchanger which provides process air with a selectable dew point required a method of controlling its coolant temperature and/or flow. The diverter valve provides the capability of controlling flow through the heat exchanger when operating with a fixed temperature coolant source, as in a spacecraft.

The diverter valve was designed with the flexibility to handle high as well as low coolant flow rates by using interchangeable valve housings having different diameter fluid connection tubes. Other valve components, including motor, drive mechanisms and electrical connections are identical. The high capacity flow diverter valve (1.6 cm (5/8 in) tube size) is used to control coolant flow through the condensing heat exchanger. The low capacity flow diverter valve (0.64 cm (1/4 in) tube size) is used to control the operating temperatures of liquid-cooled electrochemical modules, e.g., the CO_2 removal module or the O_2 generation modules.

A drawing showing the overall dimensions of the diverter valve is shown in Figure 19. Figures 20 and 21 show the assembled and partially disassembled valves, respectively. The major metal parts are machined from stainless steel. The valve spool is fabricated from Teflon. The motor and other electrical components are vendor purchased. Diverter valve weight is 0.69 kg (1.5 lb).

The diverter valve was installed in the coolant lines leading to a six-man capacity, condensing heat exchanger to verify its mechanical control capability. This was implemented by using the built-in manual adjustment capability of the valve (screw driver actuation) following removal of the drive motor. Figure 21 shows the separated flow control housing with the manual adjustment.

The electronic circuits which allow automatic feedback and control of the diverter valve were fabricated, assembled and checked out. Figure 22 is a block diagram of the electronic control circuit. The electronics were installed in the electronics cabinet of the EDC Air Supply Unit (ASU) (described below) and a checkout test of the valve and control circuitry was performed. Figure 23 is a plot of the test results. This figure shows the dew point setting on the selector knob on the front of the ASU cabinet versus process air dew point

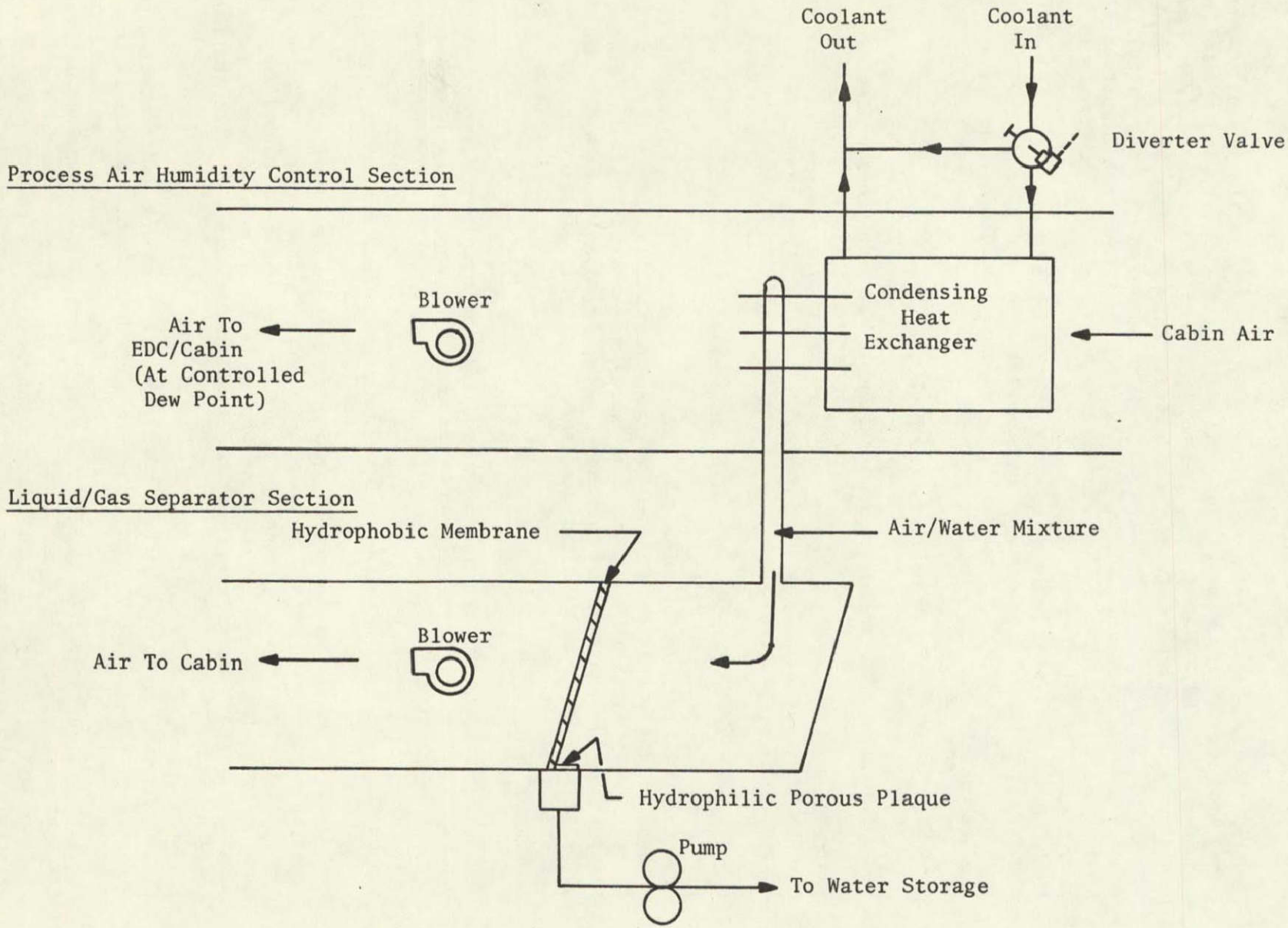
Coolant Out
Coolant In
Diverter Valve
Process Air Humidity Control Section
Blower
Air To EDC/Cabin (At Controlled Dew Point)
Condensing Heat Exchanger
Cabin Air
Liquid/Gas Separator Section
Hydrophobic Membrane
Air/Water Mixture
Blower
Air To Cabin
Hydrophilic Porous Plaque
Pump
To Water Storage

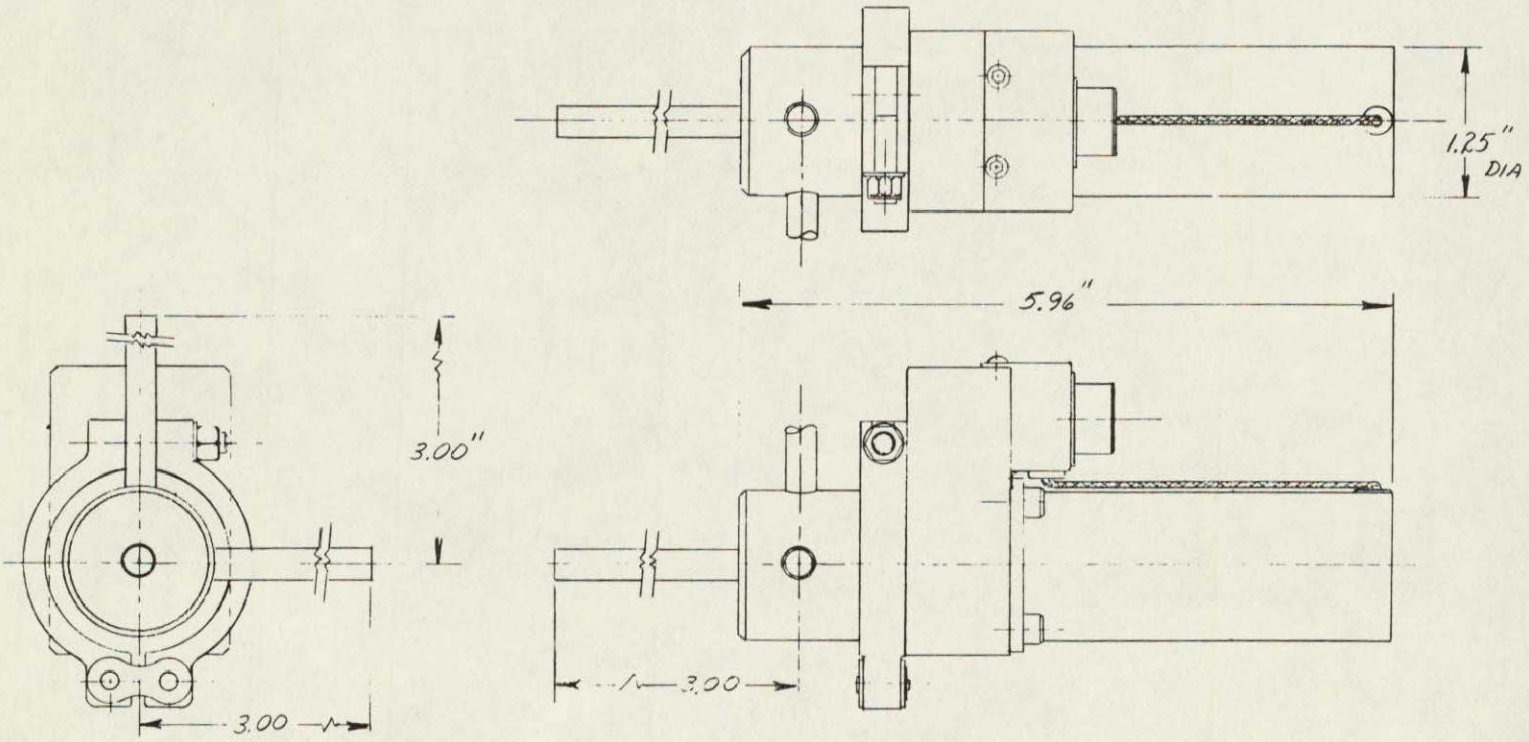

FIGURE 19 DIVERTER VALVE

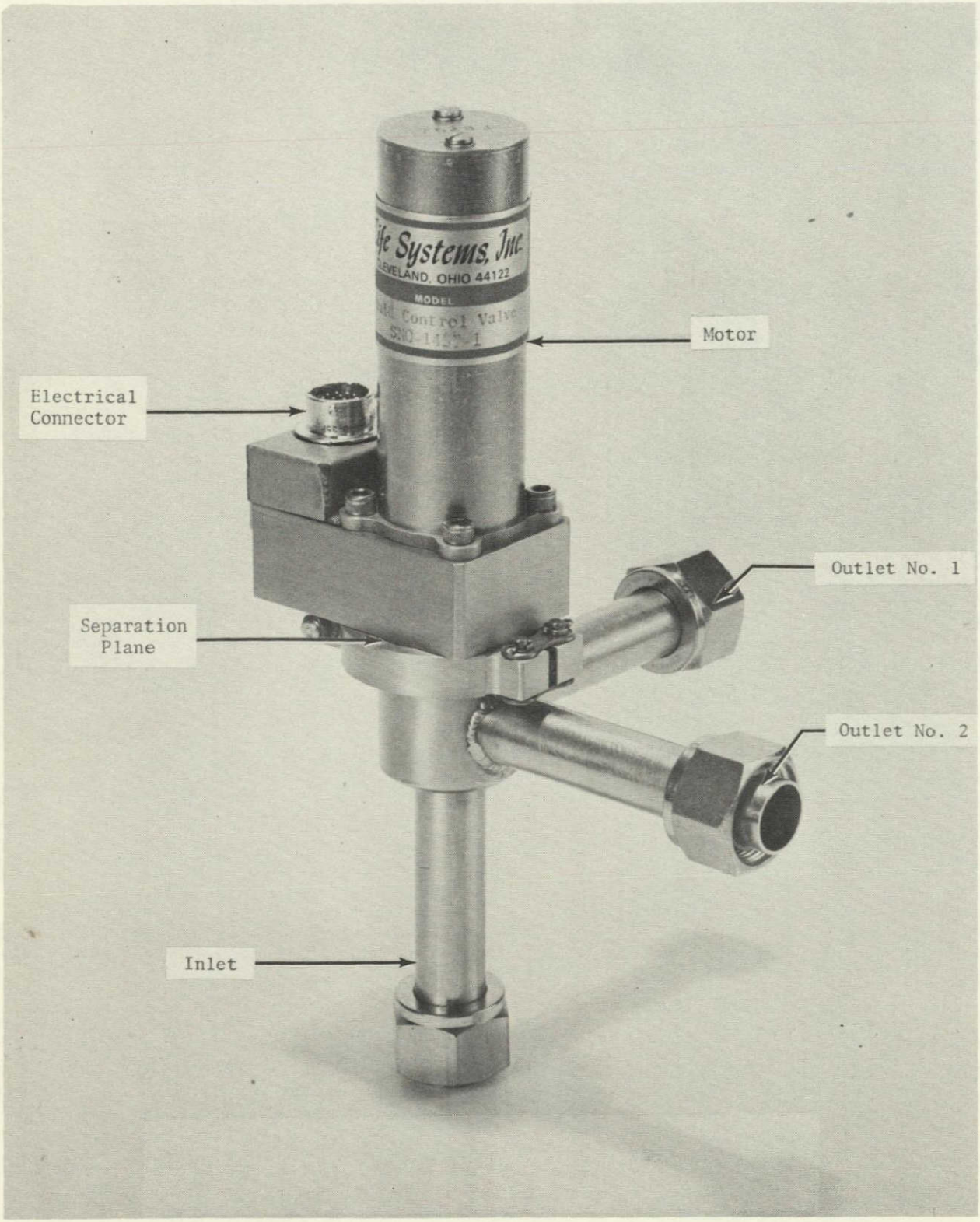

FIGURE 20 ASSEMBLED DIVERTER VALVE

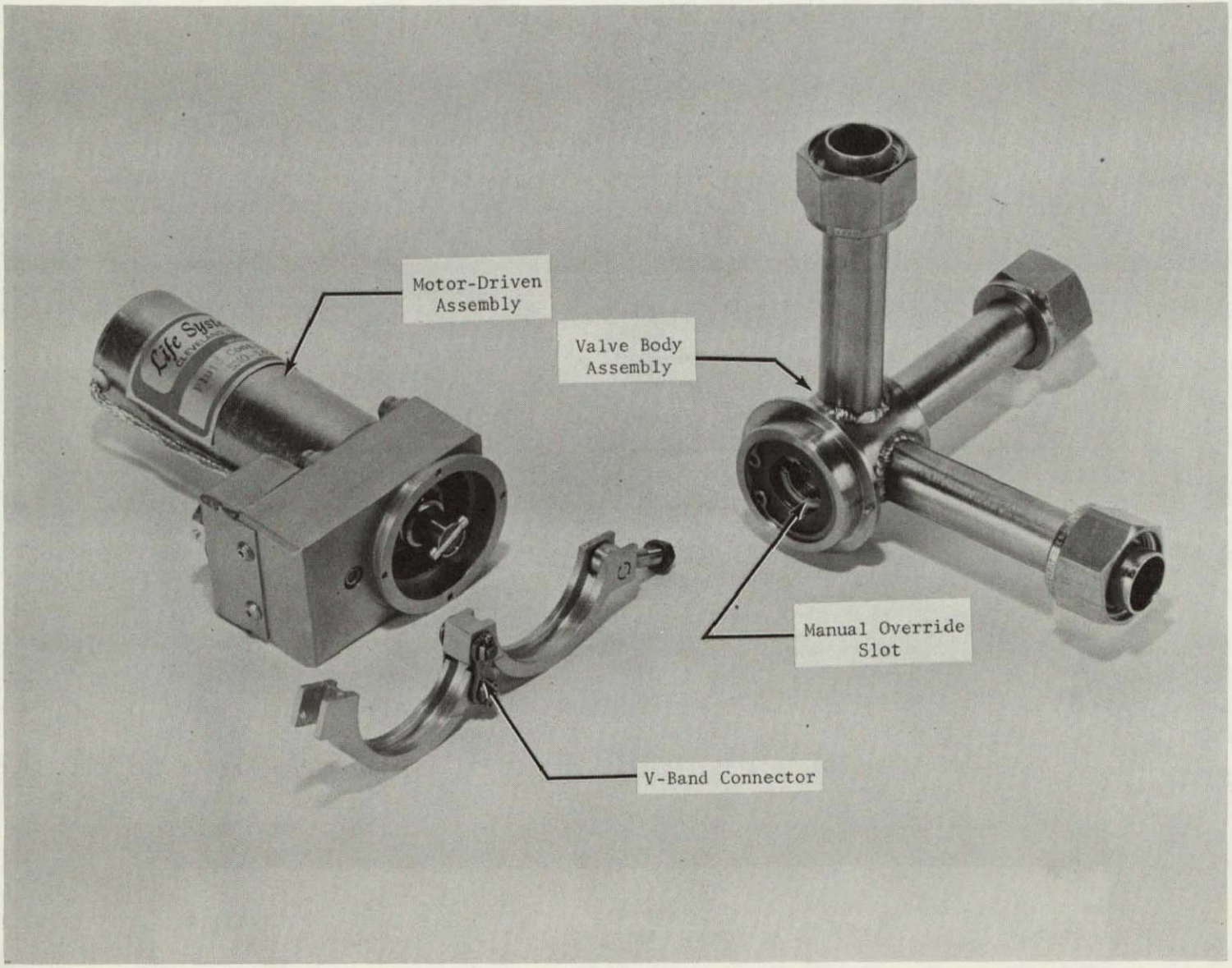

FIGURE 21 DIVERTER VALVE ILLUSTRATING MAINTAINABILITY FEATURES

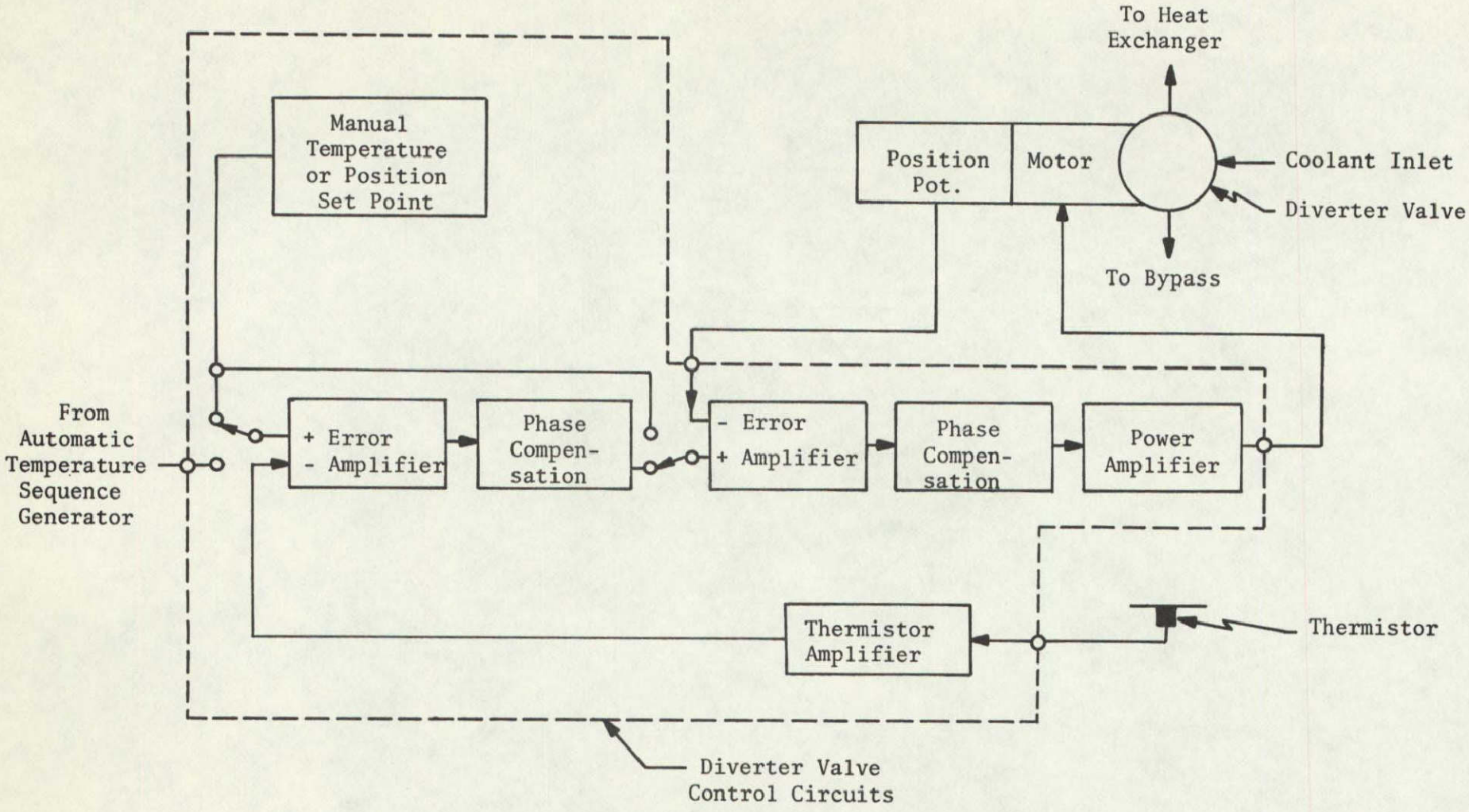

FIGURE 22 DIVERTER VALVE CONTROL BLOCK DIAGRAM

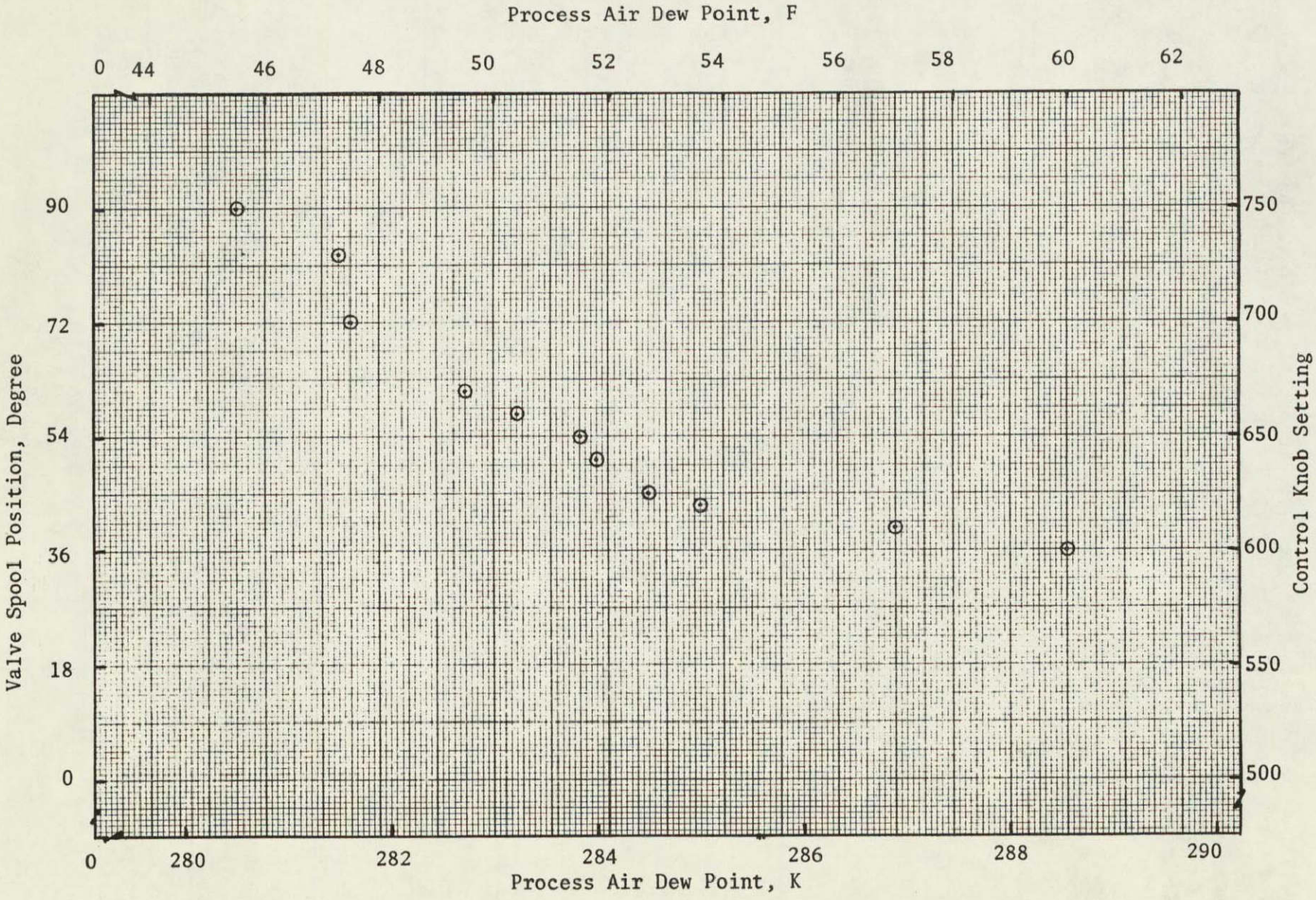

FIGURE 23 DIVERTER VALVE CHECKOUT TEST RESULTS

measured at the exit of the heat exchanger. Also plotted on the ordinate is the angular position of the diverter valve spool. Ninety degrees corresponds to the fully closed position with all coolant passing through the heat exchanger resulting in the lowest dew points. Zero degrees is equivalent to the full open or maximum bypass condition. The coolant temperature was 279 K (43.7 F). The graph shows that dew point control was achieved over a range of 281 to 289 K (45.5 to 60 F).

Condensing Heat Exchanger

The one-man condensing heat exchanger design was based on the previously established concepts used for a six-man zero gravity compatible heat exchanger. The assembled heat exchanger is shown in Figure 24. The 11.4 kg (25.0 lb) unit consists of a stainless steel support structure and an aluminum tube and fin core. Liquid coolant flows through the internal tubes which are manifolded at the ends. Process air flows perpendicular to the tubes and fins. Moisture condensing on the fins is dragged to the last row of tubes. This set of tubes/fins does not carry coolant. Rather, small diameter (0.76 mm (0.030 in)) holes are drilled into the tubes between the fins. The tubes are manifolded together and connected to a separate exit port. A blower drawing air from this port will draw a portion of the process air and all of the condensate from the tube and fin exterior surfaces, subsequently removing the condensate from the air stream. This higher quality effluent can then be more efficiently separated than from the higher flow rate, lower quality process air. The process air leaving the heat exchanger will be at a dew point temperature quite close to the coolant temperature, increasingly deviating from it as the air flow rate increases.

Liquid/Gas Separator

A zero-gravity compatible, hydrophobic membrane type liquid/gas separator was selected because of the relatively low flow and quality of the condensate mixture exiting the heat exchanger. The separator is sized for an air flow rate of 570 dm^3/min (20 cfm) and liquid flow rate of 1.7 g/min (5.35 lb/d) which corresponds to the respiration and perspiration water load for one man plus that moisture produced by a one-man EDC. Testing of the separator indicated that it could remove much higher water levels.

The separator is shown schematically in Figure 18 and pictorially in Figure 25. The principal element is a 5.1 cm x 10.2 cm (2 in x 4 in) Zitex hydrophobic membrane backed by a support screen and inclined 0.52 rad (30 deg) to the flow. Air passes through the membrane and screen. Water droplets impinge on the membrane, coalesce and are driven to the bottom of the membrane. A hydrophilic surface (nickel porous plaque) absorbs the liquid and passes it through to a small water collection chamber. A slight negative pressure on the porous plaque and continuous wetting on the chamber side is necessary for operation. A low flow liquid pump removes the water to a storage tank or accumulator. For development testing three pressure taps and a plexiglass viewing pane were included in the separator. All metal parts were machined or formed from stainless steel. The unit has a volume of approximately 2.3 dm^3 (140 in^3) and weighs 1.87 kg (4.12 lb).

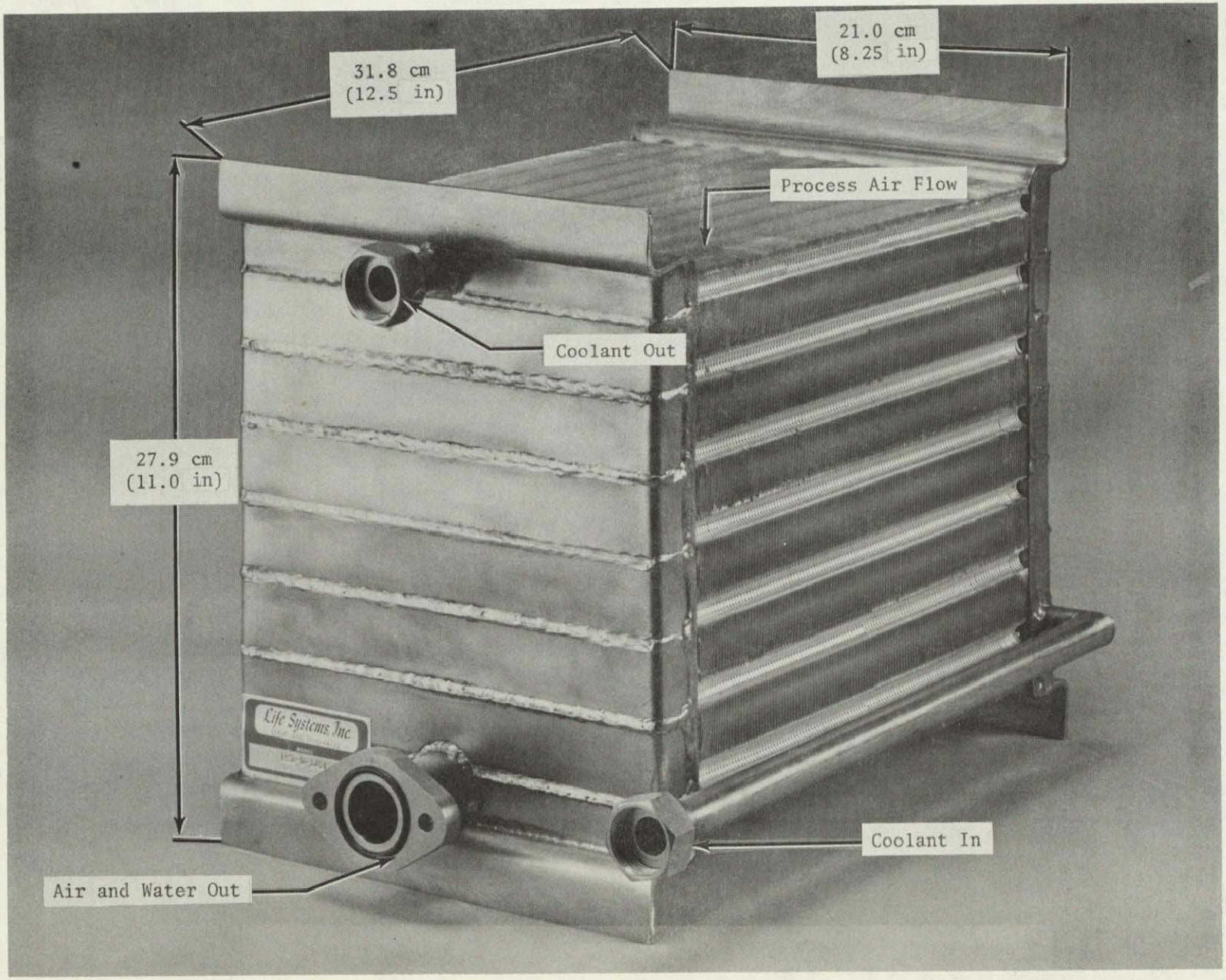

FIGURE 24 ONE-MAN CONDENSING HEAT EXCHANGER

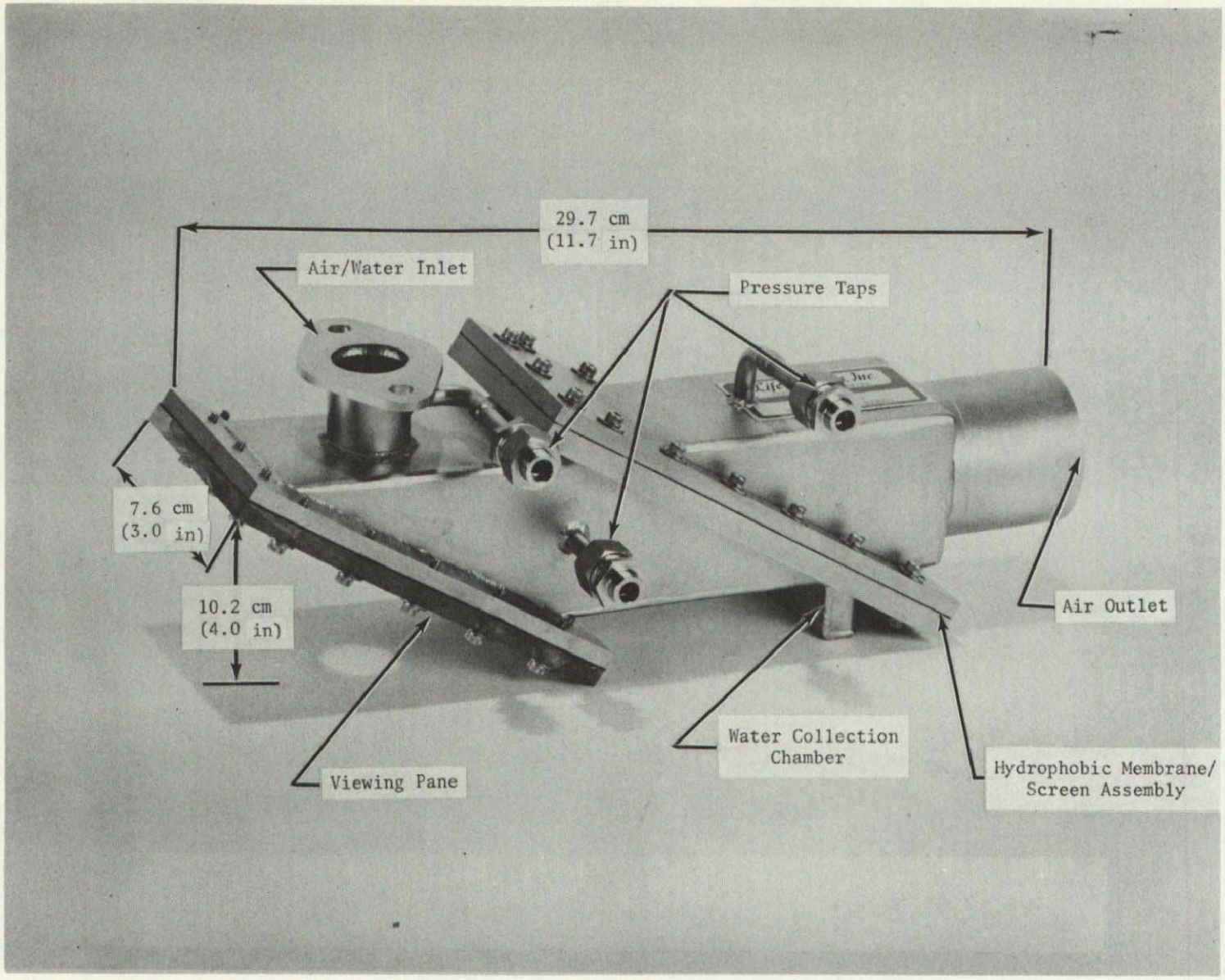

FIGURE 25 HYDROPHOBIC SCREEN LIQUID/GAS SEPARATOR

Bench testing of the assembled unit provided the flow/pressure relationship shown in Figure 26. The pressure drop across the hydrophobic membrane corresponded well with the manufacturer's specifications for the Zitex material. There were no signs of water breakthrough downstream of the membrane, even at flows exceeding 850 dm^3/min (30 cfm). Liquid behavior observations indicated that it would perform well in zero-g applications.

TEST SUPPORT ACCESSORIES DEVELOPMENTS

Test Support Accessories (TSA) were designed and developed to support the test objectives of both single cell and integrated system EDC tests. Single cell TSA supported the advanced performance level ("B" level) testing. The integrated system EDC TSA focused on developing an EDC ASU which is used to simulate a spacecraft cabin environment for EDC subsystem testing now and in the future.

Single Cell Test Stands

As part of the overall TSA support activities previously fabricated, multiposition single cell test facilities were refurbished and upgraded. Two phases of refurbishment activities were performed: initial upgrading and final refinement to meet the requirements for advanced performance level ("B" level) testing.

Initial Refurbishment and Upgrading

The single cell three-position test stand previously fabricated[5] was refurbished and upgraded to replace worn components and to increase the level of control and monitor sophistication consistent with the advancement in EDC technology.

The initial test stand had a capability to simultaneously test three different individual single cells. One of the test positions was eliminated to allow for the addition of the components and parts needed to incorporate desired improvements. Each of the two remaining positions, however, were upgraded to allow testing at the submodule level, e.g., stacking from one to five cells between one set of endplates.

The major improvement incorporated into the test facilities included upgrading the current controllers to allow for higher current operating ranges consistent with the advanced module cells, addition of provisions to allow for internally air-cooled cells and incorporation of positive feedback control of inlet process air humidity, as well as module temperature differentials (inlet dew point to outlet dry bulb temperature differential). In addition, safety shutdowns for H_2 backpressure, as well as humidity and temperature differential bands were added to the already existing cell voltage monitoring capability. Table 3 is a summary comparison of the updated test stand compared to its previous capabilities.

Advanced Level Technology Test Capability

To prepare for the advanced performance level single cell testing (described further below), additional improvements were added to the two submodule test facilities. In addition, a separate test facility was fabricated to allow for

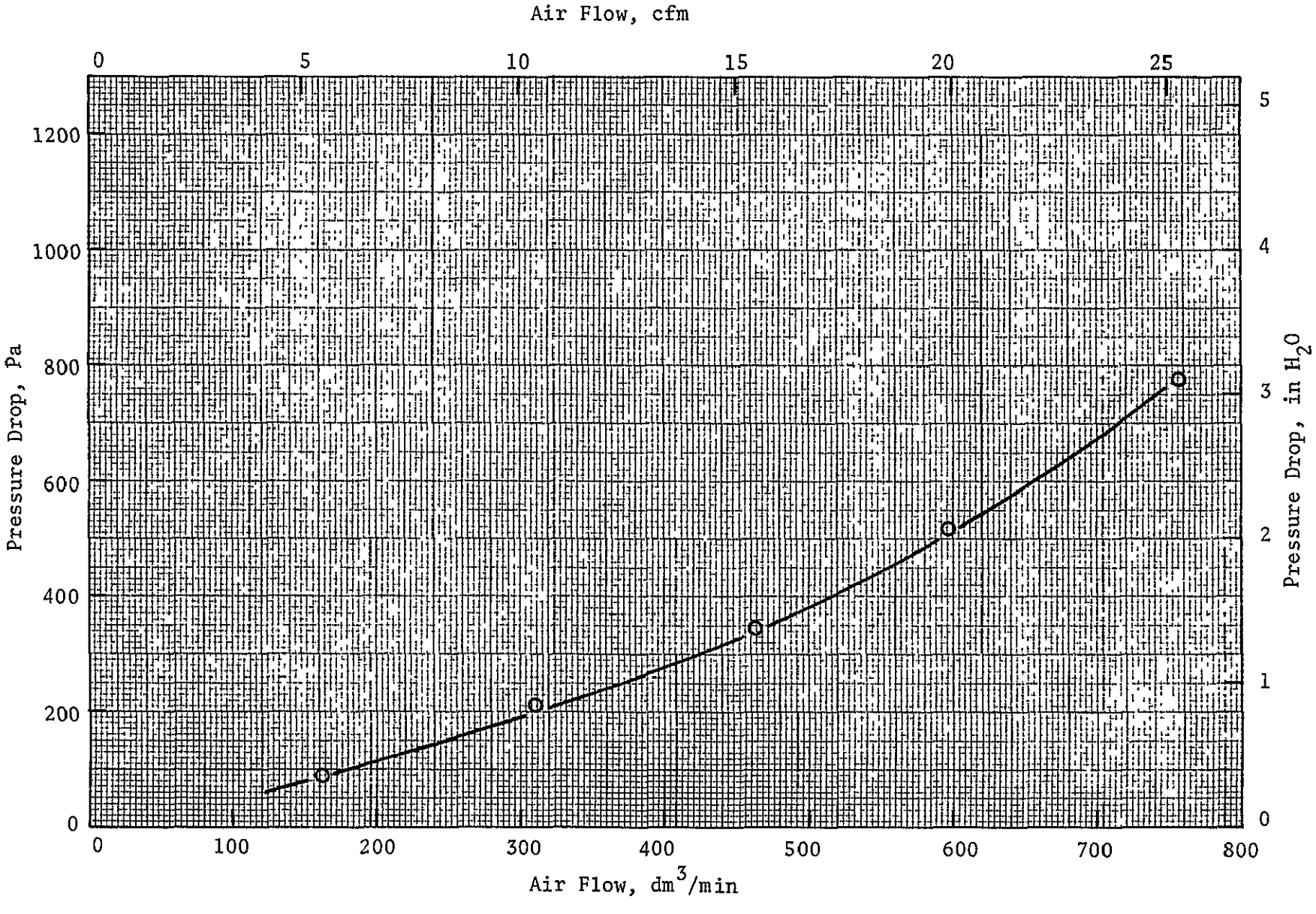

FIGURE 26 FLOW/PRESSURE CHARACTERISTICS OF LIQUID/GAS SEPARATOR

TABLE 3 SUMMARY OF SINGLE CELL TEST STAND IMPROVEMENTS

		Original Stand	Updated Stand
1.	Increased current capability	0 to 10 A	0 to 25 A
2.	Increased voltage range, negative and positive	-1.9 V to +4.5 V	-7.5 V to +7.5 V
3.	Replacement of temperature controllers	Mechanical Relays	Solid State
4.	Improved liquid coolant temperature stability	Dependent Control	Independent Control
5.	Addition of air cooling capability	Nonexistent	2 of 3 Positions
6.	Replacement of all liquid pumps	H_2O Submergeable	Nonsubmergeable
7.	Relocate and rewire electronics	Table Top Mounting	Above Test Bed Area
8.	Relocation of electrical module connections	Table Top Mounting	Above Test Area
9.	Addition of anode gas pressure shutdowns	None	1 of 3 Positions
10.	Replacement of worn valves, heaters and relays	Functional	Improved Reliability
11.	Updated process air heat exchanger	Coolant and Tape Heaters on Copper Pipe	In-line Cooling and Heating (Feedback Controlled)

continued -

Table 3 - continued

	Original Stand	Updated Stand
12. Improved control of process air dry bulb temperature	None	ΔT Control (Dry Bulb-Dew Point) or Constant Level
13. Improved module temperature control	Constant Level	ΔT Control (Dry Bulb-Dew Point) or Constant Level
14. Improved temperature sensors for control and monitor	Thermocouples	Resistance Temperature Sensors
15. Dew point temperature readout	None	Digital

simultaneous parametric testing in parallel with single cell endurance testing at the original two test positions.

The requirements of the advanced performance level testing ("B" level) were established consistent with the needs of the test program and are listed in Table 4. As Table 4 shows, the operating ranges selected are consistent with application of the EDC to projected spacecraft environments. Also, special emphasis was placed on defining and implementing automatic protection, feedback controls and operating parameter monitoring. Design and fabrication of the test facilities were completed and all requirements incorporated. Figure 27 is a functional schematic of the TSA to be used for EDC "B" level performance evaluation.

Air Supply Unit

The ASU of the EDC TSA is a closed-loop air supply and conditioning system designed to simulate the various air temperature, gas composition and humidity conditions that could be encountered in a spacecraft cabin. The ASU is used primarily to supply process and cooling air to the EDC; however, it can also be used for numerous other air treatment and air control tests.

The design approach taken was similar to standard air conditioning practice. The heart of the ASU is the contractor-provided six-man, liquid-cooled condensing heat exchanger. Process air at a dew point temperature higher than that desired is chilled to the desired dew point and subsequently post-heated to obtain the dry bulb elevation. In order to have the process air dew point above the desired level before entering the heat exchanger, water is sprayed into the loop. That, along with the moisture produced by the EDC must be above the desired saturation level in order for the design approach to work. The ASU is a single pass system in that all of the air is first chilled, then heated each pass around the loop.

The principal components of the ASU are shown schematically in Figure 28. Physically, the ASU can be divided into two parts. The first, the air processor, includes the condensing heat exchanger, circulation blower, spray chamber, spray pump, water reservoir, air heater and associated ducting, piping and support structure. These components are pictured in Figure 29 with the ASU design specifications listed in Table 5. The flow is established by the constant speed blower and the setting of the damper valves. While total circulation may be 17.0 m^3/min (600 cfm), it is possible to draw off the desired quantities of process and cooling air to the EDC. As shown in the schematic, the ASU has the capability of supplying two systems under test simultaneously.

The water is supplied to the air through a pump and spray nozzle. Excess and condensed water is gravity returned to the reservoir. The 5000 W electric heater can give a 12 K (20 F) elevation in dry bulb temperature at a nominal flow rate of 14.2 m^3/min (500 cfm). The heat exchanger also has the condensate removal capability described above for the one-man heat exchanger. This feature was provided by approximately 5000, 0.76 mm (0.030 in) holes drilled into the last rows of the heat exchanger tubes.

Aside from the sensors, all instrumentation is housed in the ASU control and monitor cabinet pictured in Figure 30. This includes the controls to operate

TABLE 4 "B" LEVEL TSA REQUIREMENTS

Number of Test Positions (Single-Cell)	3 (1 for Checkout and Parametric Tests and 2 for Endurance Tests)
Cell Hardware	Advanced Configuration
Cooling	Liquid or Air
Operating Ranges	
Current, A	0 to 20
pCO_2, Pa (mm Hg)	Ambient to 1333 (Ambient to 10)
RH, %	26 to 80
Temperature, K (F)	291 to 300 (65 to 80)
H_2 + CO_2 Backpressure, kPa (psig)	0 to 68.9 (0 to 10)
Air Flow per Cell, dm^3/s (scfm)	0 to 0.94 (0 to 2)
Automatic Protection	Low Cell Voltage High Temperature High Backpressure Low Backpressure
Controls	Constant Current Cell Temperature Inlet/Outlet Dew Point Automatic Saturator Refill
Monitor	Current Voltage Inlet/Outlet Dew Points (Air) Inlet/Outlet Temperatures (Air) Inlet/Outlet pCO_2 (Air) Outlet pCO_2 (H_2) Air Flow H_2 Flow H_2 + CO_2 Flow CO_2 Flow Inlet/Outlet Temperature (Coolant)

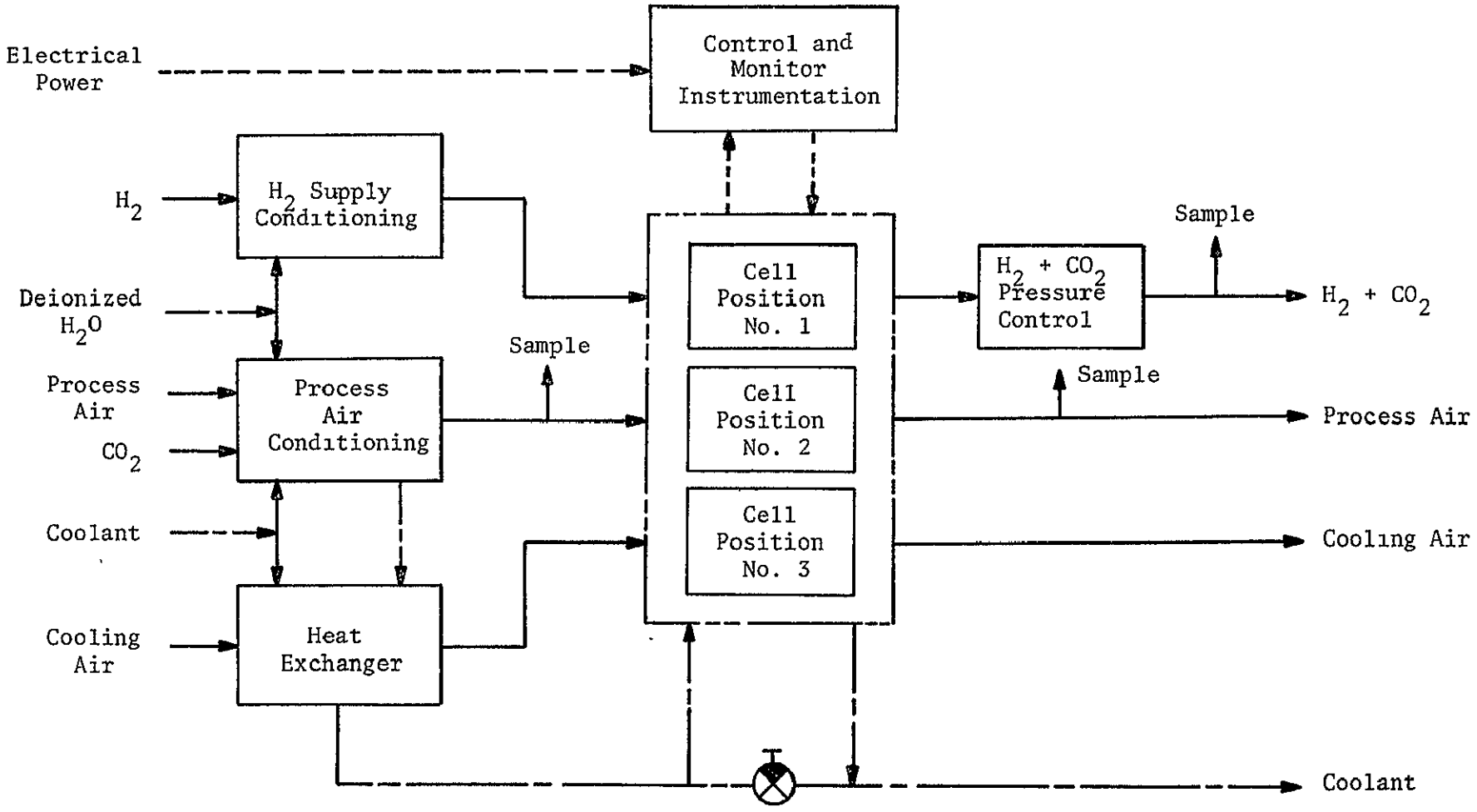

FIGURE 27 TSA SCHEMATIC FOR EDC "B" LEVEL PERFORMANCE EVALUATION

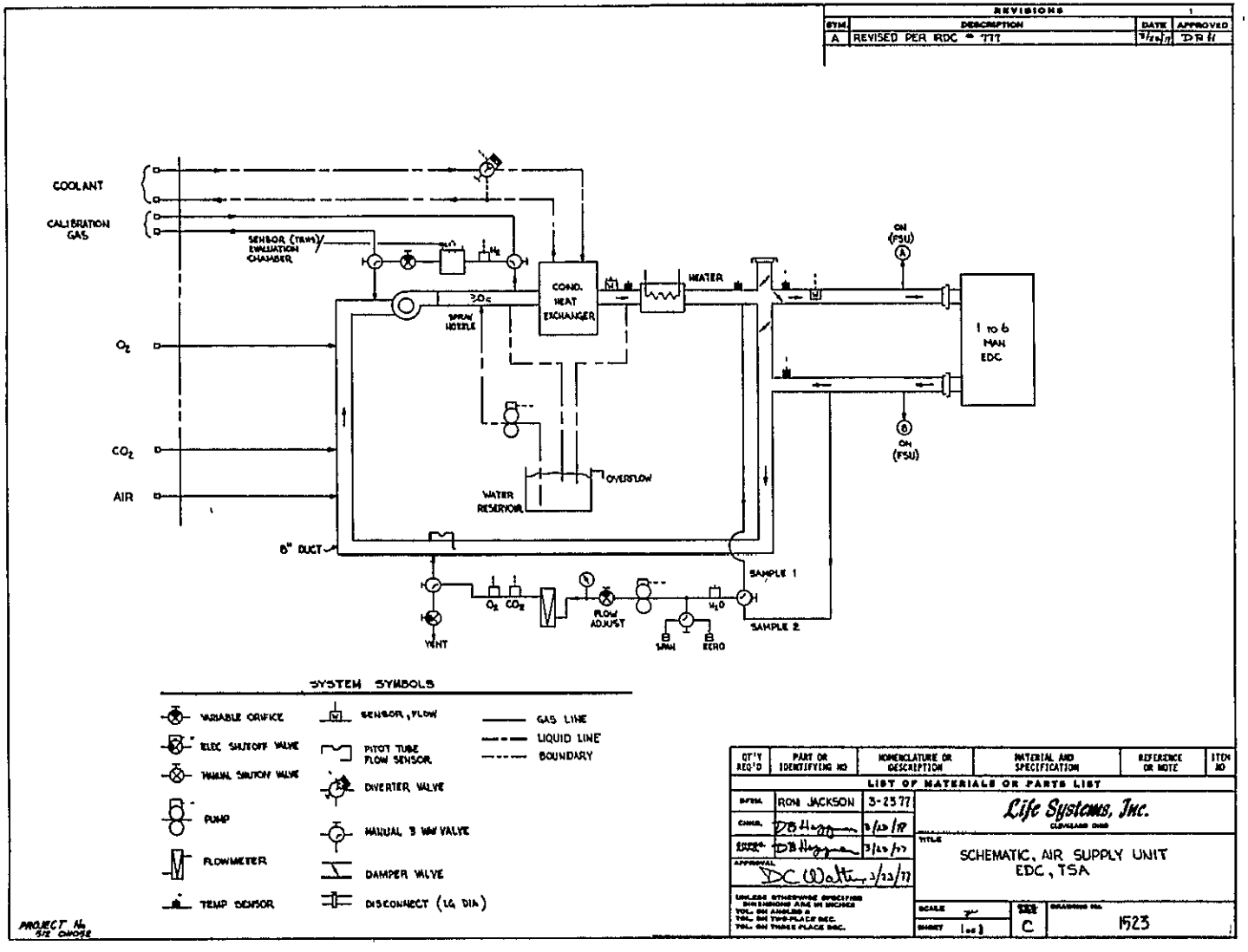

FIGURE 28 AIR SUPPLY UNIT SCHEMATIC

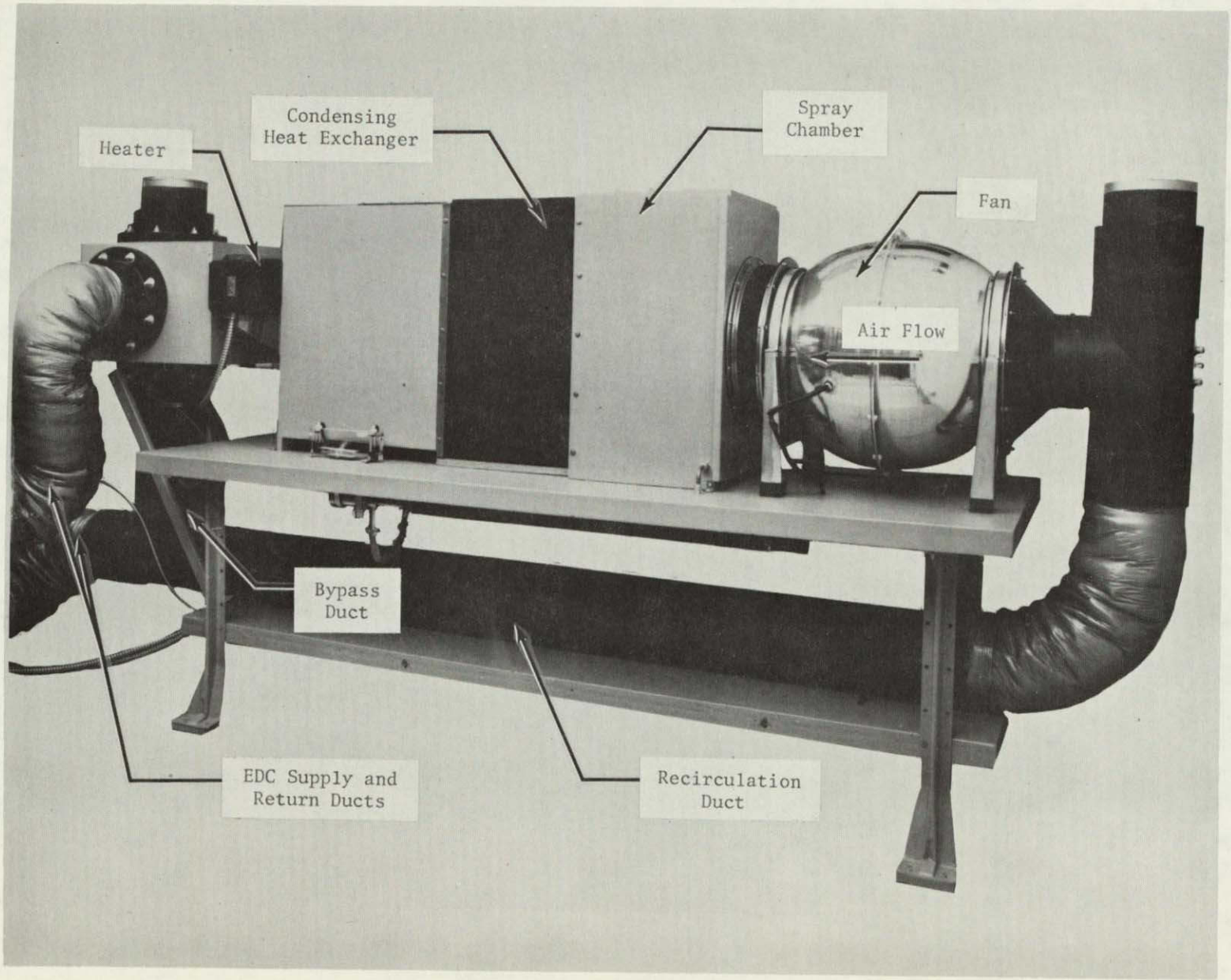

FIGURE 29 AIR SUPPLY UNIT

TABLE 5 ASU DESIGN SPECIFICATIONS

Crew Size	6 Men
Processed Air	
Flow Rate, m^3/min (scfm)	0 to 17.0 (0 to 600)
Dew Point Range, K (F)	279 to 301 (42.5 to 82)
Dry Bulb Range, K (F)	279 to 302 (42.5 to 85)
Humidity Range, %	26 to 100
Condensing Heat Exchanger	
Heat Removal Capacity, kJ/s (BTU/h)	6.0 (20,500)
Effectiveness	0.905
Coolant	
Flow Rate, dm^3/s (gpm)	0.4 (6)
Temperature, K (F)	277 (40)
System Pressure	
Nominal, kPa (psia)	101 (14.7)
Deviation, kPa (in H_2O)	$\pm$0.74 ($\pm$3)
Nominal Gas Composition, kPa (mm Hg)	
O_2	21.3 (160)
CO_2	0 to 0.93 (0 to 7)
H_2	0.76 (5.7)
N_2	Makeup
Physical	
Air Processor	
Size, WxDxH, m (ft)	3.4x0.91x1.8 (11 x 3 x 6)
Envelope Volume, m^3 (ft^3)	5.7 (200)
Weight, kg (lb)	273 (600)
Power, W	6500
Control and Monitor Cabinet	
Size, WxDxH, m (ft)	0.55x0.67x1.8 (1.8 x 2.2 x 6.0)
Envelope Volume, m^3 (ft^3)	0.65 (23)
Weight, kg (lb)	114 (250)
Power, W	1000

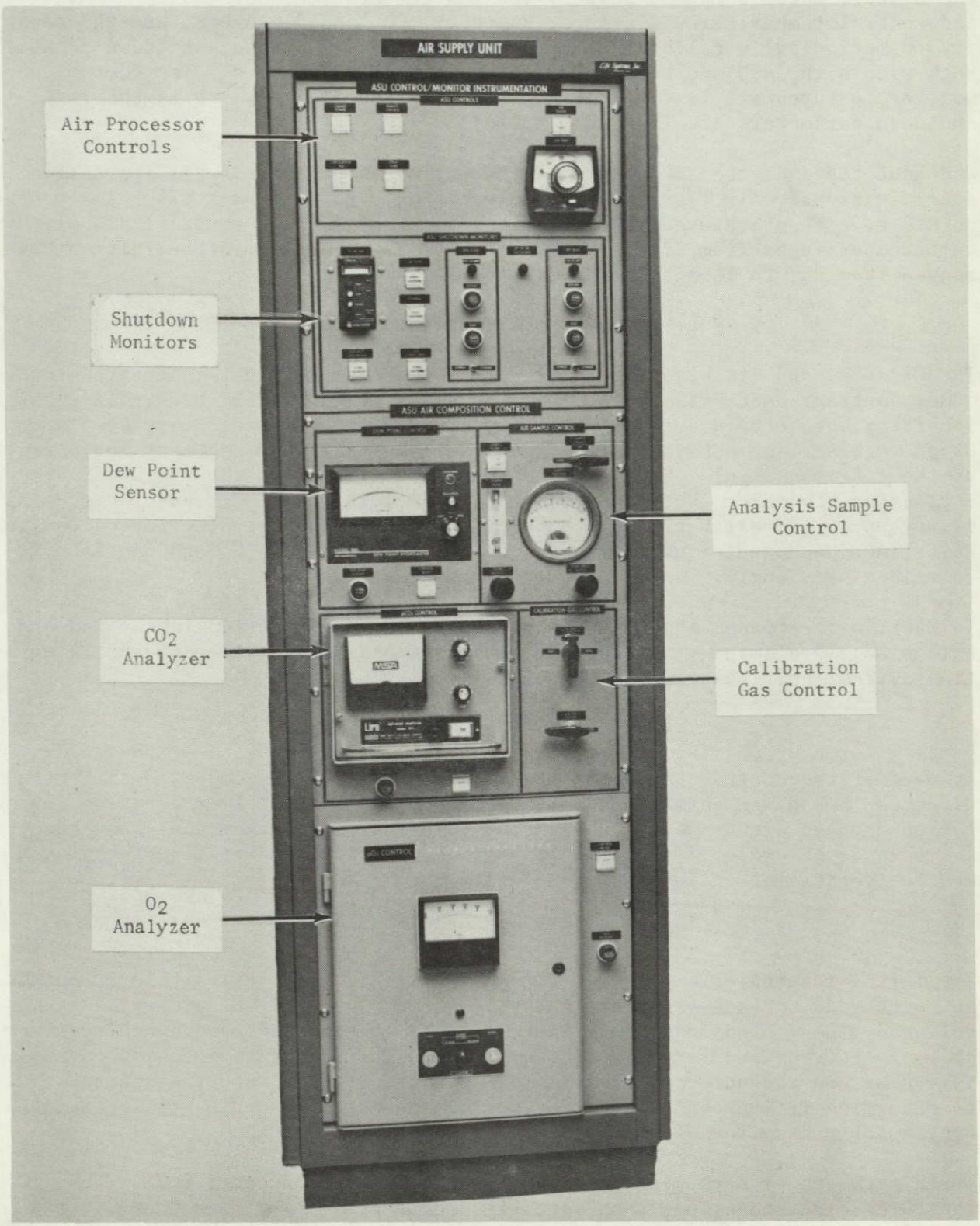

FIGURE 30 ASU CONTROL AND MONITOR INSTRUMENTATION

the blower, water pump and heater; the instrumentation and sensors to monitor and control temperature, pressure, humidity, CO_2 and O_2 levels; and the capability to periodically calibrate the instruments. In addition, shutdown capability both within the ASU and to and from other subsystems exists. The control and monitor features are listed in Tables 6 and 7 respectively, while the five shutdown parameters are listed in Table 8.

Checkout tests of the ASU indicated that it meets or exceeds all its design specifications. Air flows are in the range of 0 to 20 m^3/min (750 cfm). Dew points have been achieved in the range 279 to 301 K (42.5 to 82 F) and dry bulb temperatures from 279 to 302 K (42.5 to 85 F). Relative humidities have ranged from 26% to 100% saturation.

Four-Man Laboratory Breadboard Support

The CXA-4(A) and its associated TSA was assembled to support integrated testing under Contract NAS8-30891. This test system, termed the LBS-B/ORS-4(A), was a laboratory breadboard system consisting of a Bosch Reduction Subsystem, an Oxygen Reclamation Subsystem (ORS) and the EDC integrated together and operating at the four-man level. Figure 31 is the block diagram of the LBS-B/ORS-4(A) indicating the three subsystems and their TSA. The EDC TSA consisted of modifications to the existing Fluid Supply Unit (FSU) and Test Accessories Control Unit (TACU) and additions of a new Coolant Supply Unit (CSU) and the ASU described previously.

To date, all elements shown in Figure 31 have been purchased, fabricated and assembled. Preliminary testing indicates successful operation of the integration system, particularly the CXA-4(A) and its TSA.

TECHNOLOGY ADVANCEMENT STUDIES

As part of the contractual effort four studies have been completed that were directed toward the advancement of EDC technology. These four areas of investigation were an electrode Teflon loading study, a performance deviation study, scale up of hardware of a previously developed matrix fabrication technique and the definition of advanced EDC performance level goals.

Electrode Teflon Loading Study

The Teflon loading, i.e., the Teflon percentage in the catalyst binder on the EDC electrode surface, significantly affects CO_2 removal efficiency and cell voltage. The Teflon loading of the electrode controls the hydrophobic nature of the electrode and results in altering the electrode gas diffusion layer thickness and the number of available reaction sites. A study was conducted to determine if improvements in EDC performance were possible by altering the Contractor's baseline electrode Telfon loading.

Three cathodes with varying amounts of Teflon were fabricated and tested. Of the three electrodes, one contained the previously established Contractor's baseline Teflon composition, one contained a 10% lower than baseline loading, while the third contained a 10% higher than baseline Teflon composition. The electrodes were mounted and parametrically tested in standard CS-6 EDC single cells with internal air cooling.

TABLE 6 ASU CONTROL PARAMETERS

PCO_2

A CO_2 analyzer samples the air stream and measures pCO_2 in the range 0 to 0.93 kPa (0 to 7 mm Hg). The output of the analyzer drives a pCO_2 electronic controller which actuates a series of controlled orifices which permit controlled amounts of CO_2 to enter the closed system. The pCO_2 can be a selectable constant value or a preprogrammed periodic variation.

pH_2O

The output of the dew point sensor controls a diverter valve attached to the heat exchanger coolant lines. The diverter valve alters the flow of coolant through the heat exchanger permitting control of dew point.

pO_2

The O_2 analyzer output signal actuates a solenoid valve that controls flow of O_2. The pO_2 remains at desired level (nominally 21%, 21.3 kPa (160 mm Hg)).

Air Temperature

Air temperature (dry bulb) is sensed by a thermocouple. The thermocouple drives a heater controller which adjusts the current to the electric duct heater.

Total Air Pressure

a. Overpressurization controlled by air leaks and blowout parts.

b. Underpressurization controlled by a low ΔP pressure regulator and tank source of makeup air.

Air Flow Rate

Air flow sensed by pitot and turbine flow sensors. Flow is controlled by adjustment of orifices in EDC and bypass ducts.

TABLE 7 ASU MONITOR PARAMETERS

Parameter	Instrument	Readout
pCO_2	LIRA IR Analyzer	Meter - % CO_2, Calibration Curve
pH_2O	Cambridge Dew Point Sensor/Analyzer	Meter - F, Dew Point Temperature
pO_2	Beckman Model F3 O_2 Analyzer	Meter - % O_2
Air Temperature	Type K Thermocouple	Meter - F, Heater Controller
Air Pressure	Pressure Gauge - 2 Stations	Meter - $\pm$ in H_2O
Air Flow Rate	1. Pitot Tube/Inclined Manometer	Gauge - Calibration Curve to CFM
	2. Turbine Flow Meter	Meter - CFM
Flow Indicator	AFS Air Flow Monitor	On/Off for Shutdown Control
pH_2	General Monitors Model 180	Meter - % H_2 Alarm for Shutdown

TABLE 8 ASU SHUTDOWN PARAMETERS

Dry Bulb Temperature

Set Point - In the range 283 to 319 K (50 to 114 F)
Band - Set Point 0 to ±3.6 K (±6.4 F)

Dew Point Temperature

Set Point - In the range 272 to 307 K (30 to 94 F)
Band - Set Point 0 to ±3.6 K (±6.4 F)

Air Flow

Air flow sensor/switch detects (by pressure) when air flow decreases to zero and opens a pair of normally closed relay contacts.

Hydrogen

Alarm at 1% H_2 concentration, shutdown at 2% H_2 concentration in circulating gas stream.

External Shutdown

External signal from other subsystems causes a shutdown of the ASU.

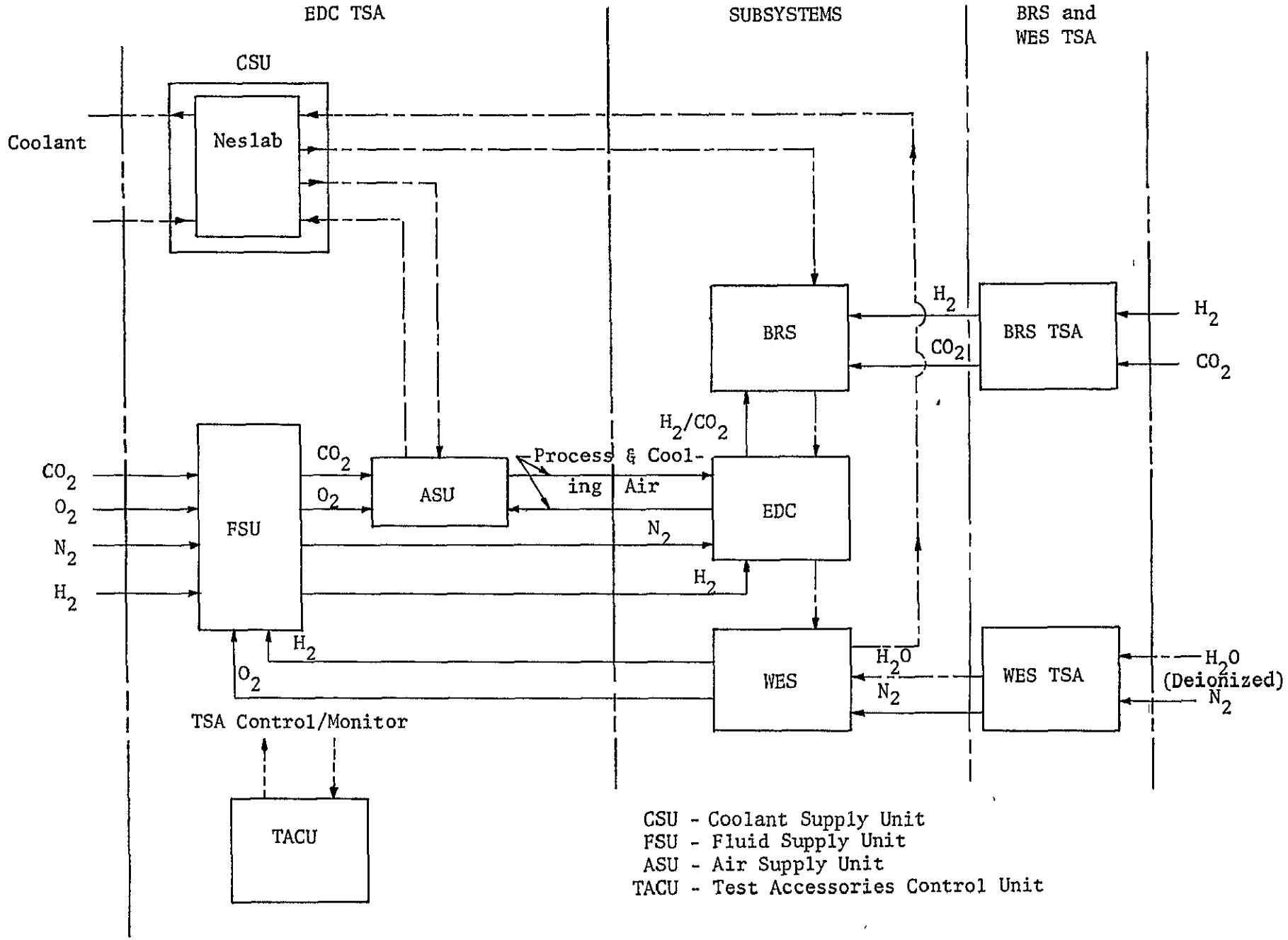

FIGURE 31 LBS-B/ORS-4(A) BLOCK DIAGRAM SHOWING RELATIONSHIP BETWEEN TSA AND SUBSYSTEMS

The results of the testing are shown in Figures 32 and 33 which illustrate the CO_2 removal and voltage performance of the three cathodes as a function of inlet pCO_2 level and current density, respectively.

The 10% higher than baseline Telfon electrode exhibited poor CO_2 removal efficiency and extremely poor electrical performance, failing to maintain a positive voltage and caused an early termination of the test. The 10% lower The 10% higher than baseline Teflon electrode exhibited poor CO_2 removal efficiency and extremely poor electrical performance, failing to maintain a positive voltage and caused an early termination of the test. The 10% lower than baseline Teflon electrode, while exhibiting a removal efficiency slightly less than baseline, did show a higher than normal cell voltage.

From these tests it can be concluded that the optimum Teflon loading for CO_2 removal occurs at the baseline loading while a cell more optimized for power output (higher cell voltage) would require a composition slightly less than baseline but greater than the low Teflon electrode tested, i.e., approximately 5% less than baseline loading.

Performance Deviation Study

During past EDC developments certain cells exhibited deviations from the expected baseline performance, i.e. subnormal CO_2 removal and electrical efficiencies. These same cells also exhibited distributions of CO_2 removal, water evolution and dry bulb temperature increases over the surface area of the electrode. A performance deviation study was conducted to analytically and experimentally investigate the observed maldistributions. First, the study examined previous test data, and second the data was analyzed to identify a mechanism which could result in the subnormal CO_2 removal and electrical efficiencies.

Review of Previous Data

Representative data was selected from previous experiments. This data was categorized with respect to specific cell configurations and/or cell operating conditions. Samples of air-cooled as well as internally liquid-cooled cells were chosen to investigate possible influences of the cooling technique used.

Figure 34 shows CO_2 concentration and dew point profiles obtained with a CS-6 style cell which had demonstrated subnormal CO_2 removal and voltage performance. The data illustrates poor CO_2 removal in the middle portion of the electrode area. Typically, the middle portion of this cell style with its externally air-cooled fins will operate at an above average temperature and a below average RH. These operating conditions result from the temperature gradients required to remove the cell's product heat through the external fin. The data points towards a maldistribution of current density exemplified by the lack of dew point gained and by the low CO_2 removal in the air stream flowing over the middle section of the cell.

Data obtained from an advanced liquid cooled cell (AEDC) is plotted in Figure 35. This figure is a plot of the percent CO_2, dew point and dry bulb temperatures of the process air exiting the individual ports of the advanced cell frame. The cell ports are numbered 1 through 16 and correspond to the rectangular

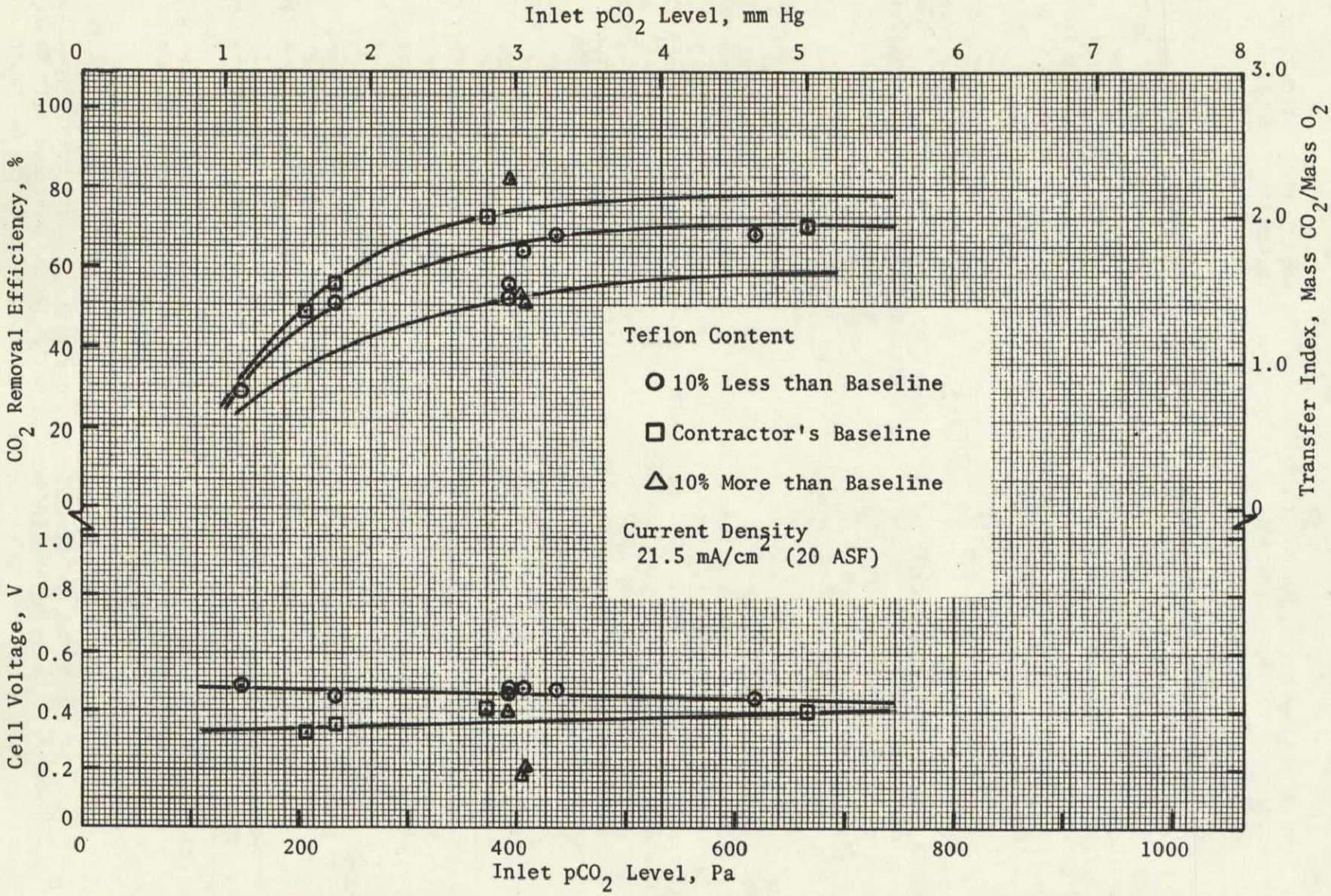

FIGURE 32 EDC PERFORMANCE AS A FUNCTION OF PROCESS AIR pCO_2 FOR VARIABLE TEFLON LOADING LEVELS

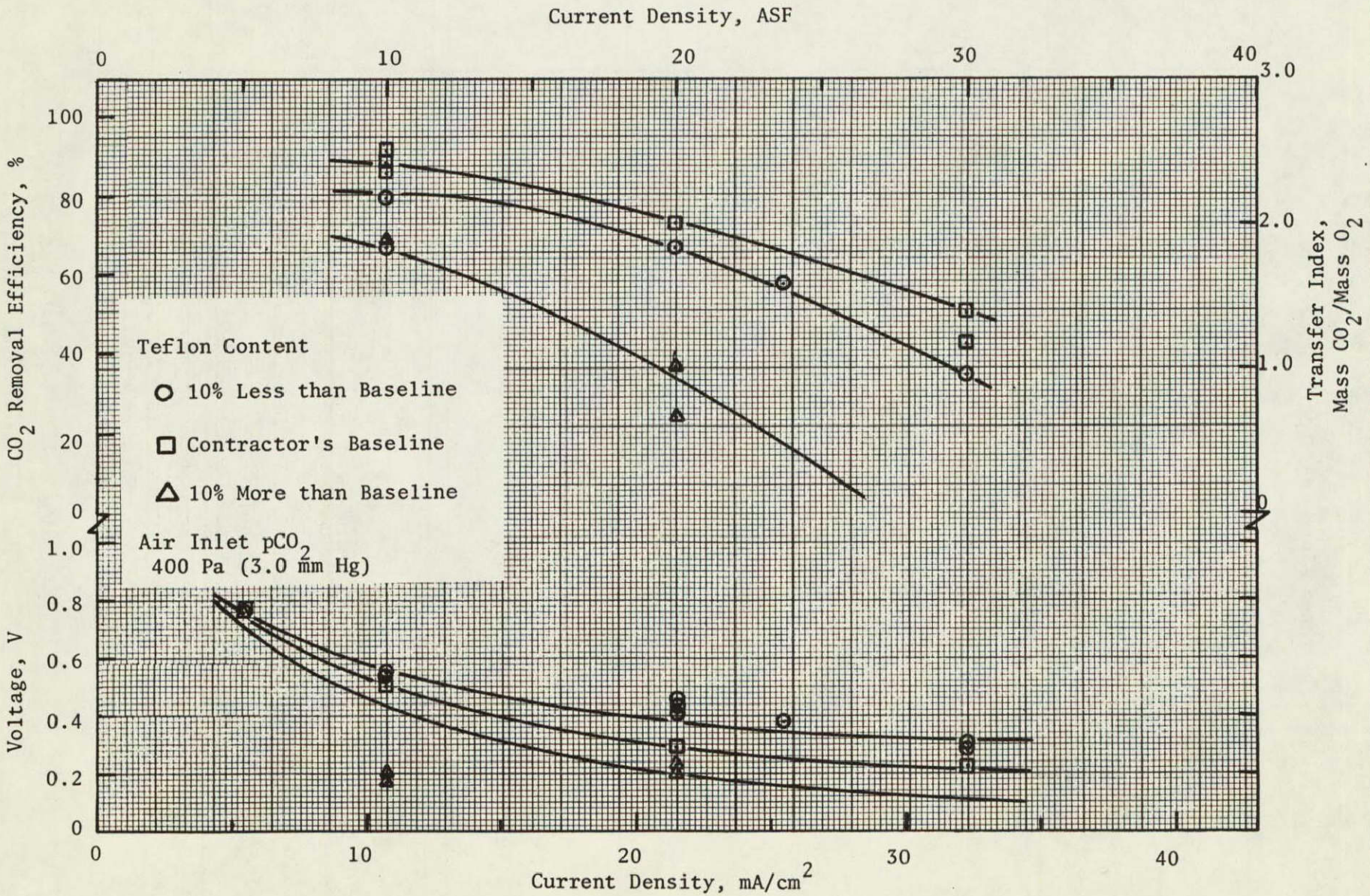

FIGURE 33 EDC PERFORMANCE AS A FUNCTION OF CURRENT DENSITY FOR VARIABLE TEFLON LOADING LEVELS

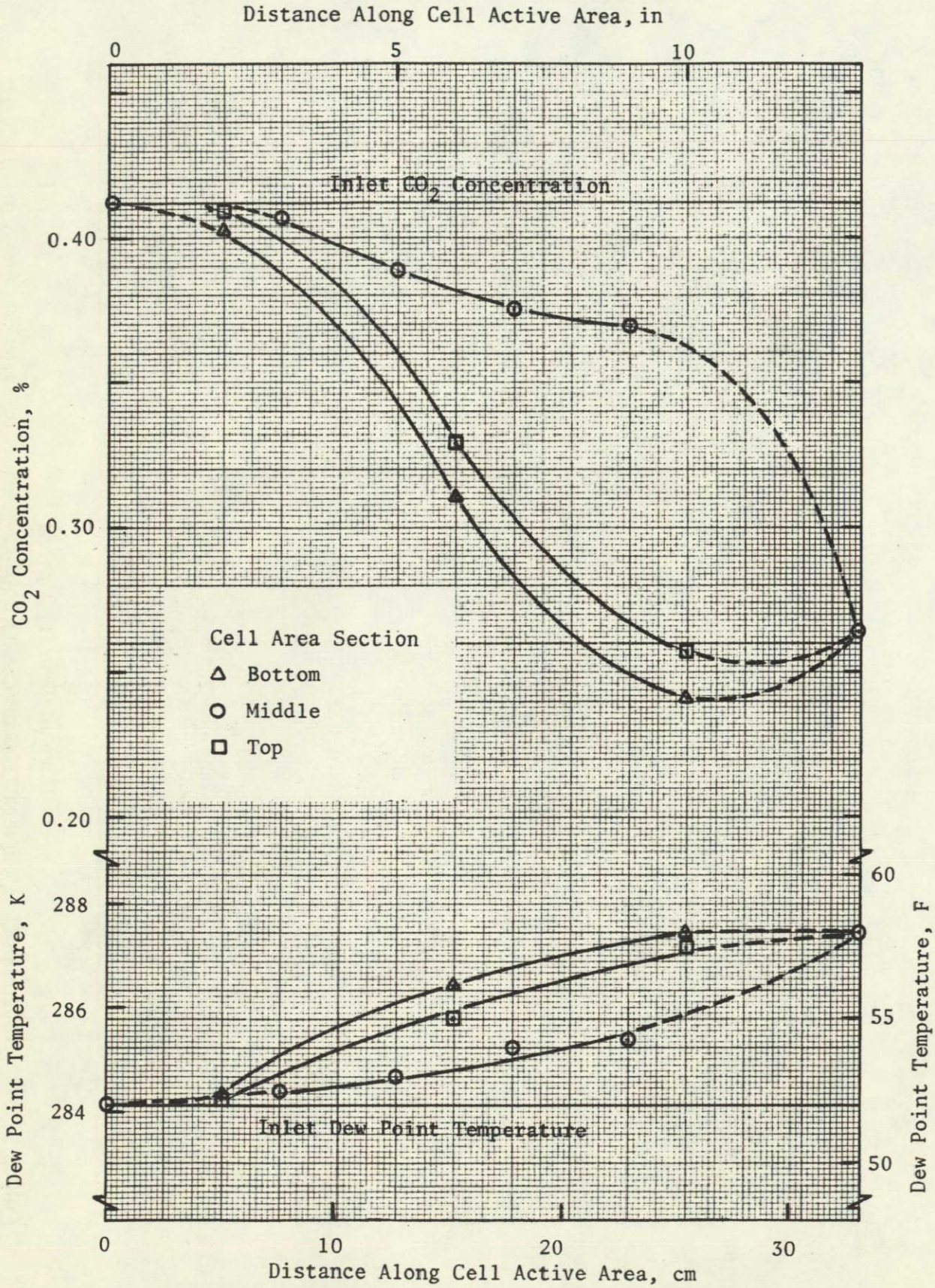

FIGURE 34 CO_2 AND DEW POINT PROFILES FOR EDC CELL EXHIBITING SUBNORMAL PERFORMANCE

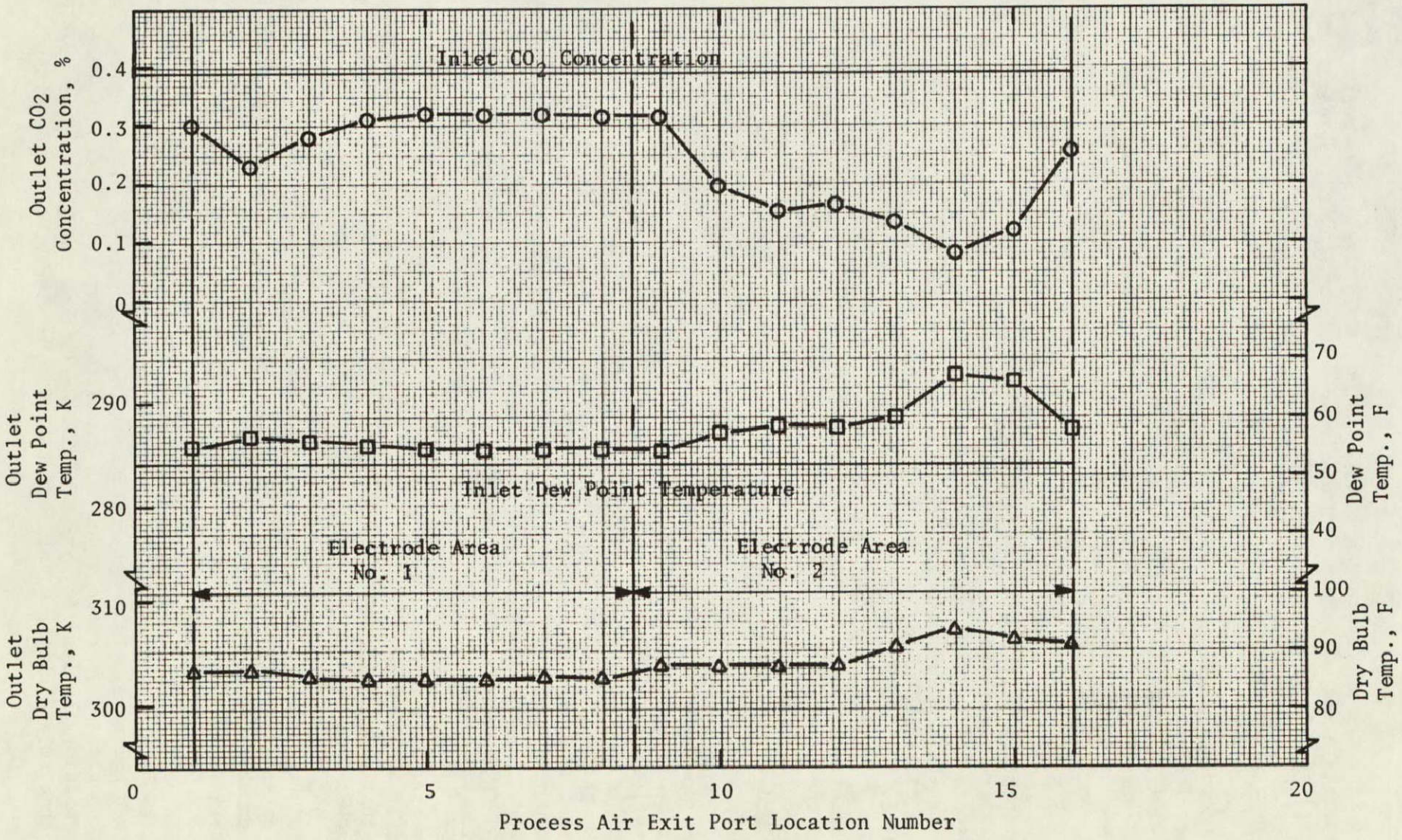

FIGURE 35 EXIT PROCESS AIR PROFILES FOR AEDC LIQUID-COOLED CELL EXHIBITING SUBNORMAL PERFORMANCE

openings through which process air exits the cell frame. The openings of the two separate electrode areas of the advanced EDC design are represented by numbers 1 through 8 and 9 through 16, respectively. The overall performance of the AEDC liquid-cooled cell was poor as reflected by its CO_2 removal and electrical efficiencies. The figure illustrates the difference in performance of the two electrode areas; one exhibiting seemingly low CO_2 removal rates while the other indicated high or normal CO_2 removal rates. The elevated water evolution rates and dry bulb temperature increases correspond to that portion of the cell (exit ports 9 through 16) that showed the high CO_2 removal rate. These results again indicate a current maldistribution between the two electrode areas.

Electrolyte Precipitation Mechanism

The performance deviations observed in previous test data, as discussed above, illustrate current density maldistribution. The current density maldistribution observed in the testing cannot be explained from the normal maldistributions which result from internal cell resistance variations. The mathematical modeling of the EDC CO_2 transfer process identified a HCO_3^- precipitation mechanism.[12,13] The model evaluated the effects of process air RH, flow rate and pCO_2 level, current density and cell operating temperature and identified these factors as controlling the anolyte HCO_3^- concentration. An illustration of the effects of the two major parameters, current density and process air RH, on the anolyte HCO_3^- concentration is presented in Figure 36. This figure shows the increase in anolyte concentration as current density and RH decrease.

If, for some combination of reasons, the electrolyte concentration exceeds its solubility level, the precipitate formed can cause partial masking of the cell's effective area to current transport. This partial masking can result in blockage of H_2 and O_2 or increased resistance to ionic transport. An area which is partially masked decreases in active current density. Figure 36 shows that this decrease in current density will result in additional anolyte salt formation and accelerate the electrode masking process. As an electrode is masked, the current density of the remaining active region of the electrochemical cell increases resulting in areas of high CO_2 removal and water evolution as observed in the test data. With the effective current density increase, the performance levels of both CO_2 removal and electrical efficiencies is decreased as has been shown by baseline EDC performance at high current densities. This mechanism would result in the performance deviations observed in the testing and relates these deviations to the electrolyte HCO_3^- precipitation mechanism proposed.

Several factors can contribute to the initial salt formation. These factors can be external or operation-related parameters. Large temperature gradients have been observed and reported for the CS-6 style external fin cooled cells.[10,14] Other factors could be flow distribution of gases, internal cell resistances, elevated pCO_2 levels, compression of electrode surfaces, out-of-tolerance operation or dry ambient air purging of a non-operating EDC. Which exact factors cause the initial salt formation in the previous test data cannot be determined but once a cell has initiated a masking process of the electrode surface, decreases in current density result at that area. With these current density maldistributions an operating EDC will enter the electrolyte precipitation mechanism and continue until a steady-state situation has developed.

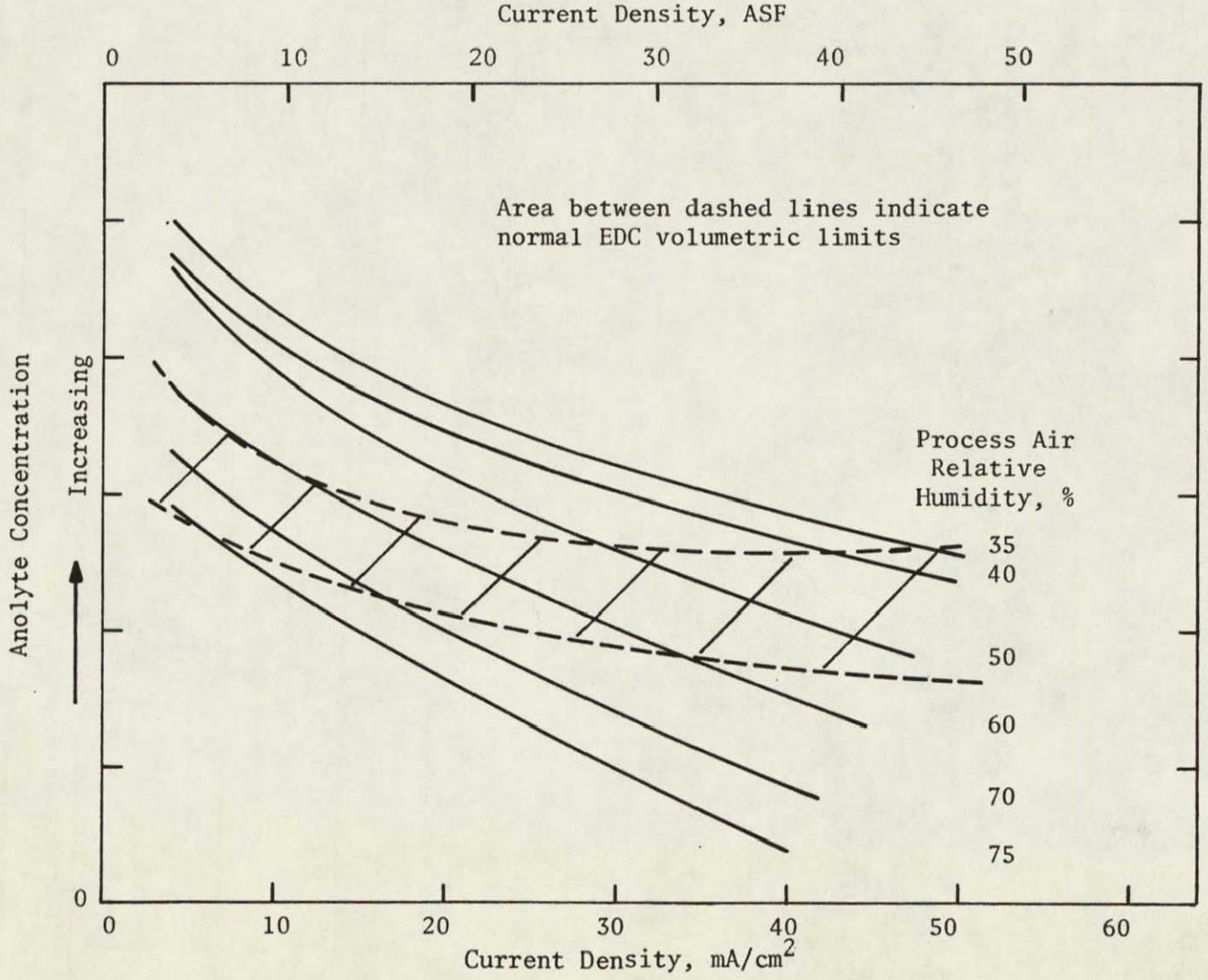

FIGURE 36 ILLUSTRATION OF THE EFFECTS OF CURRENT DENSITY AND RELATIVE HUMIDITY ON ANOLYTE CONCENTRATION

Three corrective actions can be taken to prevent the observed performance deviations. Initially, a cell design which eliminates large temperature gradients and the potential for entering the electrolyte precipitation mechanism is desirable. This change has occurred in LSI technology through the introduction of the internally liquid and internally air cooled AEDC cells. A second modification would be the selection of an electrolyte which would maximize both $CO_3^=$ and HCO_3^- solubility levels and decrease the potential from entering the electrolyte precipitation mechanism. The third requirement is that non-operating EDCs need to be isolated from ambient conditions to prevent purging with dry ambient air and contact with excessively high pCO_2 levels.

Matrix Fabricator

Previously used fuel cell grade asbestos matrices are no longer commercially available. For this reason LSI had previously defined a step-by-step procedure for fabricating reconstituted fuel cell grade asbestos matrices from commercially available raw asbestos fibers. A matrix fabricator was required to verify the procedure at the scaled-up lecel required by full sized EDC cells.

Based on the matrix manufacturing procedure requirements a new asbestos matrix fabricator was designed. A drawing detailing the fabricator design is shown in Figure 37. The unit is of a welded aluminum construction to resist deterioration due to fluids used during the matrix fabrication procedure. The fabricator utilizes a rubber gasketed porous nickel (Ni) plaque to support the matrix material during the vacuum deposition phase.

Performance Level Definition

An "A" level of EDC performance had been established as a goal prior to the development of the one-man[5] and the six-man[6] EDC's. To date, the "A" level performance has been demonstrated and exceeded. To advance the technology further and to achieve performance improvements, more stringent goals must be established. Therefore, "B" level performance goals were derived and adopted as standards for subsystem level performance.

The "B" level performance goals had been demonstrated at various times but only on a single cell level. A comparison of the "A" and "B" level performance is presented in Figures 38 and 39. The operating conditions for Figures 38 and 39 are shown in Table 9. The "B" level of performance on a multi-cell level is projected to be demonstrated under a follow-on task of Contract NAS2-8666.

CONCLUSIONS

The following conclusions are a direct result of the program studies.

1. A five-cell liquid-cooled AEDCM operating at 30 mA/cm^2 (28 ASF) with the 4.6 dm^2 (0.50 ft^2) advanced cells can remove the CO_2 metabolically generated by one man. High cell voltages (0.4 V) and CO_2 transfer efficiencies (76%) have been demonstrated over a 30-day endurance test.

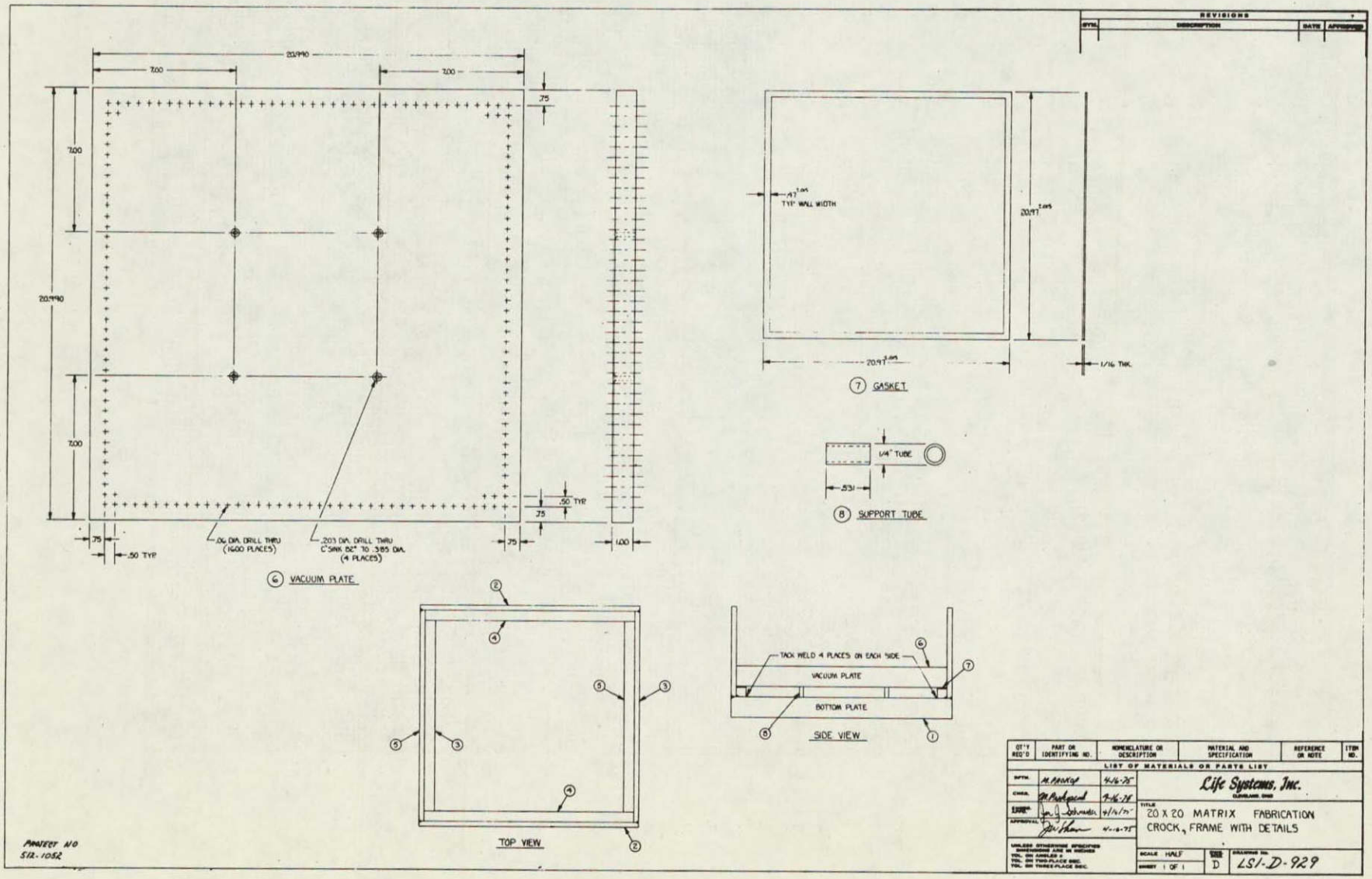

FIGURE 37 ASBESTOS MATRIX FABRICATOR DESIGN

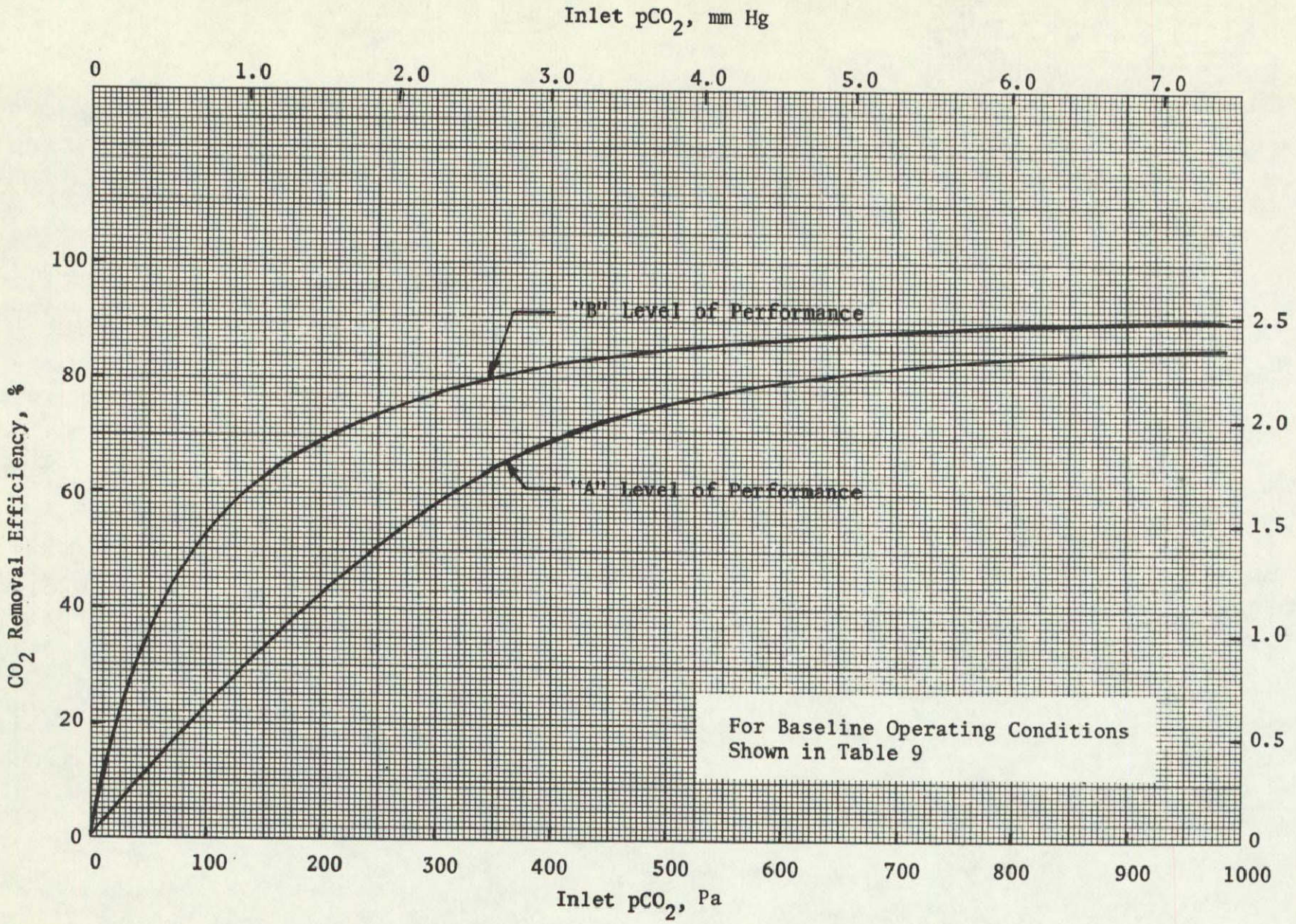

FIGURE 38 COMPARISON OF "A" AND "B" LEVEL OF EDC PERFORMANCE (INLET pCO_2)

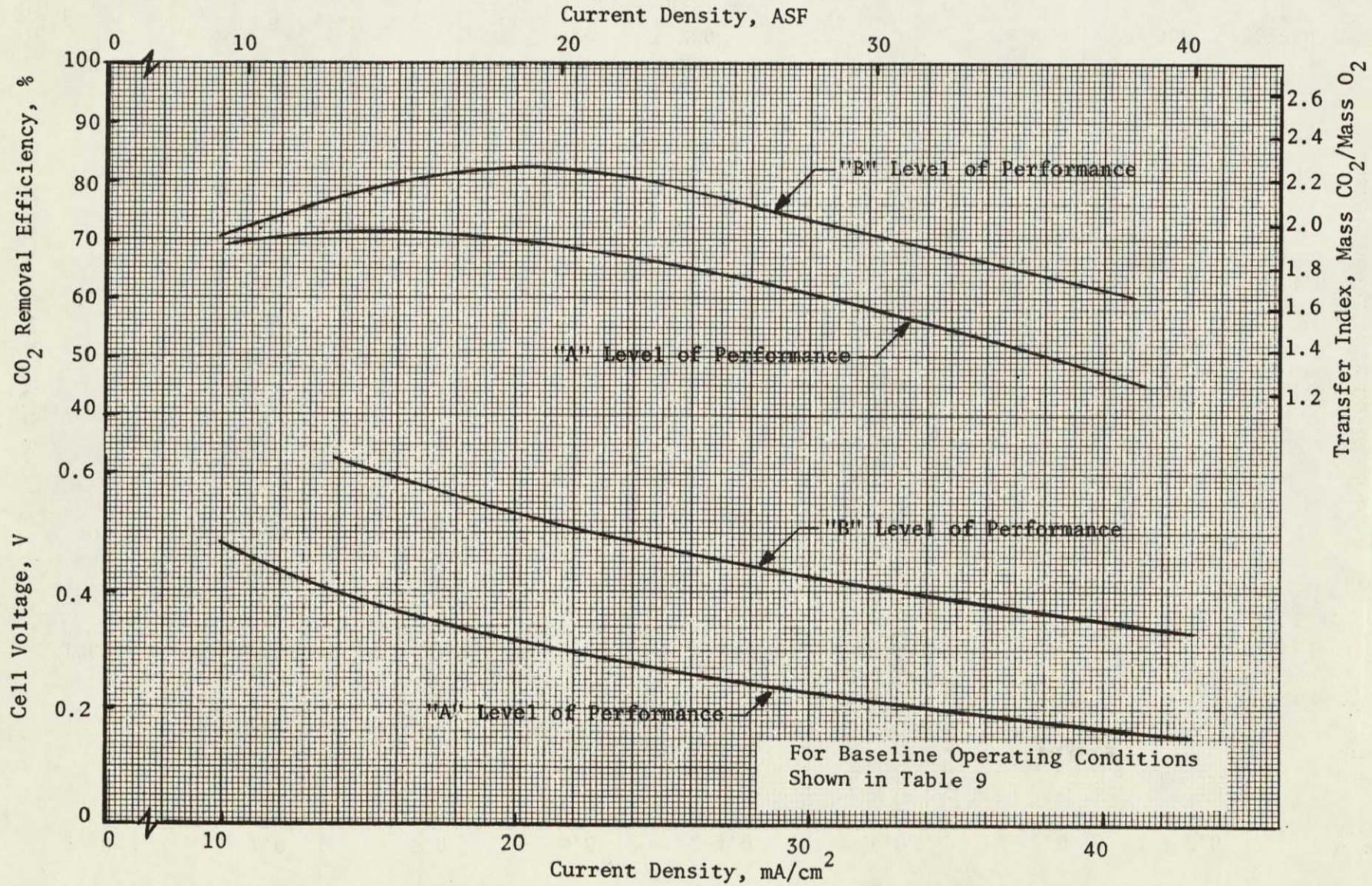

FIGURE 39 COMPARISON OF "A" AND "B" LEVEL OF EDC PERFORMANCE
(CURRENT DENSITY)

TABLE 9 BASELINE OPERATING CONDITIONS
FOR "A" AND "B" PERFORMANCE LEVEL COMPARISONS

pCO_2, Pa (mm Hg)	400 (3.0)[a]
Current Density, mA/cm^2 (ASF)	21.5 (20)[b]
Air Flow/Cell[c], dm^3/s (scfm)	0.75 (1.60)
Inlet Process Air Temperature, K (F)	294 ±3 (70 ±5)
Inlet RH, %	
"A" Level	70 to 80
"B" Level	50 to 60
H_2 + CO_2 Backpressure, Pa (psig)	Ambient

(a) Variable for Figure 38
(b) Variable for Figure 39
(c) For a 0.045 m^2 (0.488 ft^2) active cell area

2. The electrochemical CO_2 removal concept can be readily integrated with an OGS and either a S-CRS or a BRS with only a minimum number of interface components and using state-of-the-art hardware. No problems have been identified with using OGS generated H_2 in the EDC, nor either of the CRSs using the EDC exhaust gases.

3. The capability for operating air EDC directly with a varying spacecraft environment in terms of CO_2 and humidity loading conditions now exists. This capability is provided by the development of several humidity control subsystem components including diverter valves, heat exchangers and two types of liquid/gas separators.

4. A closed loop spacecraft cabin environment simulator capability exists which will permit long duration testing of future EDC subsystems. This ASU can cover a wide range of environmental conditions including changing temperature, humidity, CO_2 and O_2 levels.

5. An electrolyte precipitation mechanism has been hypothesized to explain apparent current density maldistributions in EDC cells which are associated with subnormal CO_2 removal and electrical efficiencies. Understanding of this mechanism permits corrective action to be taken in future cell designs which will alleviate the performance deviations that have been noted in the past.

6. Electrode Teflon loading studies have indicated that the optimum Teflon loading is at or near the baseline cell construction presently being used. Relatively minor changes in cell performance would be obtained by either increasing or decreasing the Teflon loading.

RECOMMENDATIONS

The following recommendations are a direct result of the program's conclusions.

1. Integration technology of an EDC with an OGS and a Bosch and/or Sabatier-type CO_2 reduction process has been demonstrated. The next step of integration technology should incorporate the EDC and its specialized components (i.e., diverter valve, liquid/gas separators, heat exchangers, etc.) with other EC/LSS subsystems into an ARS. Emphasis should be placed on process control, process dynamics and "real world" variations of operating conditions. This total ARS approach would save development costs, further establish subsystem technology and acquire the techniques of interfacing hardware to enable isolated subsystems to operate as one system. Test Support Accessories and testing costs would also be saved when several subsystems are operated together. This approach should be established at the one-man level initially.

2. Experiments should be performed to establish a new advanced level ("B") of EDC technology. This effort should focus on increasing cell voltage (to greater than 0.5 V) and on increasing CO_2 removal efficiency in spite of decreasing process air flow rate or pCO_2 level. This new technology should include improved catalyst Teflon binder configuration, high quality electrode matrices and optimum

electrolyte compositions. The activities for developing the new "B" level of technology should include extensive endurance testing (up to 120 days) to establish the confidence in the new performance level.

REFERENCES

1. Samonski, F. H. and Neel, J. M., "Atmosphere Revitalization for Manned Spacecraft - An Assessment of Technology Readiness," presented at the 24th Congress, Baku USSR, October, 1973.

2. Quattrone, P. D., "Spacecraft Oxygen Recovery System" Astronautica Acta 18, No. 4, pp. 261-272, October, 1973.

3. Quattrone, P. D., Babinsky, A. D. and Wynveen, R. A., "Carbon Dioxide Control and Oxygen Generation," presented at the ASME Conference, Paper No. 70-AV/SpT-8, Los Angeles, CA, June 21-24, 1970.

4. Wynveen, R. A. and Quattrone, P. D., "Electrochemical Carbon Dioxide Concentrating System," presented at the SAE/ASME/AIAA Conference, Paper No. 71-Av-21, San Francisco, CA, July 12-14, 1971.

5. Wynveen, R. A., Schubert, F. H. and Powell, J. D., "One-Man, Self-Contained CO_2 Concentrator System," Final Report, Contract NAS2-6118, NASA CR-114426, Life Systems, Inc., Cleveland, OH, March, 1972.

6. Powell J. D., Schubert, F. H., Marshall, R. D. and Shumar, J. W., "Six-Man, Self-Contained Carbon Dioxide Concentrator Subsystem," Final Report, Contract NAS2-6478, NASA CR-114743, Life Systems, Inc., Cleveland, OH, June, 1974.

7. Kostell, G. D., Schubert, F. H., Shumar, J. W., Hallick, T. M. and Jensen, F. C., "Six-Man, Self-Contained Carbon Dioxide Concentrator Subsystem for Space Station Prototype (SSP) Application," Final Report, Contract NAS2-6478, NASA CR-114742, Life Systems, Inc., Cleveland, OH, May, 1974.

8. Schubert, F. H. and Quattrone, P. D., "Development of a Six-Man, Self-Contained Carbon Dioxide Collection Subsystem for Spacecraft Application," Paper No. 74-ENAs-16, Intersociety Conference on Environmental Systems, Seattle, WA, July, 1974.

9. Winnick, J., Marshall, R. D. and Schubert, F. H., "An Electrochemical Device for Carbon Dioxide Concentration, I. System Design and Performance," I&EC Process Design and Development, Volume 13, pp. 59-63, January, 1974.

10. Schneider, J. J., Schubert, F. H., Hallick, T. M. and Woods, R. R., "Electrochemical Carbon Dioxide Concentrator Advanced Technology Tasks," Final Report, Contract NAS2-6478, CR-137732, Life Systems, Inc., Cleveland, OH, October, 1975.

11. Schubert, F. H., Quattrone, P. D. and Clark, D. C., "Integrated Testing of an Electrochemical Depolarized CO_2 Concentrator (EDC) and a Bosch CO_2 Reduction Subsystem (BRS)," Paper 76-ENAs-35, Intersociety Conference on Environmental Systems, San Diego, CA, July, 1976.

12. Lin, C. H. and Winnick, J. "An Electrochemical Device of Carbon Dioxide Concentration II. Steady-State Analysis, CO_2 Transfer," Ind. Eng Chem. Process Des. Develop., 13 (1), 1974.

13. Lin, C. H., Heineman, M. L and Angus, R. M. "An Electrochemical Device of Carbon Dioxide Concentration II. Steady-State Analysis, Energy and Water Transfer," University of Missouri, Columbis, MO, 1973.

14. Marshall, R. D., Schubert, F. H. and Carlson, J. N., "Electrochemical Carbon Dioxide Concentrator: Math Model," Final Report, Contract NAS2-6478, CR-114639, Life Systems, Inc., Cleveland, OH, August, 1973.